



ALMA MATER STUDIORUM
UNIVERSITÀ DI BOLOGNA

Neutron induced cross section measurements

Cristian Massimi

Department of Physics and Astronomy & INFN

Outline:

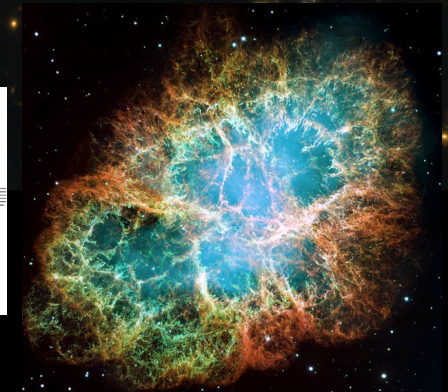
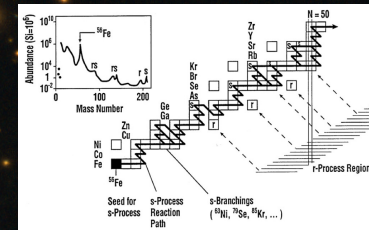
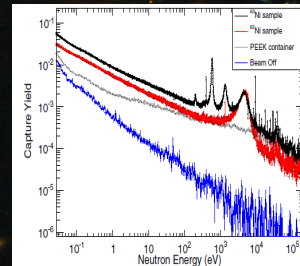
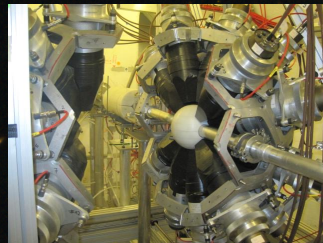
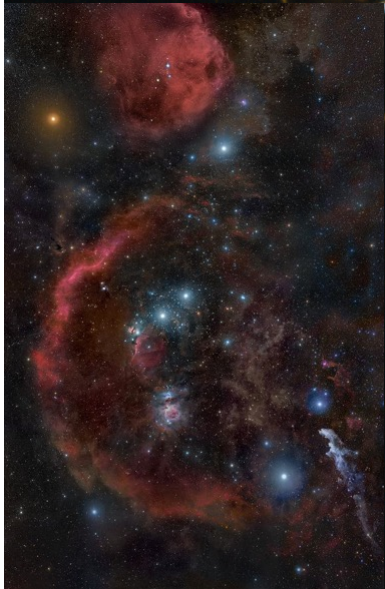
- n_TOF @ CERN 
- MACS
- Examples of measurements and their impact on Nuclear Astrophysics

Outline



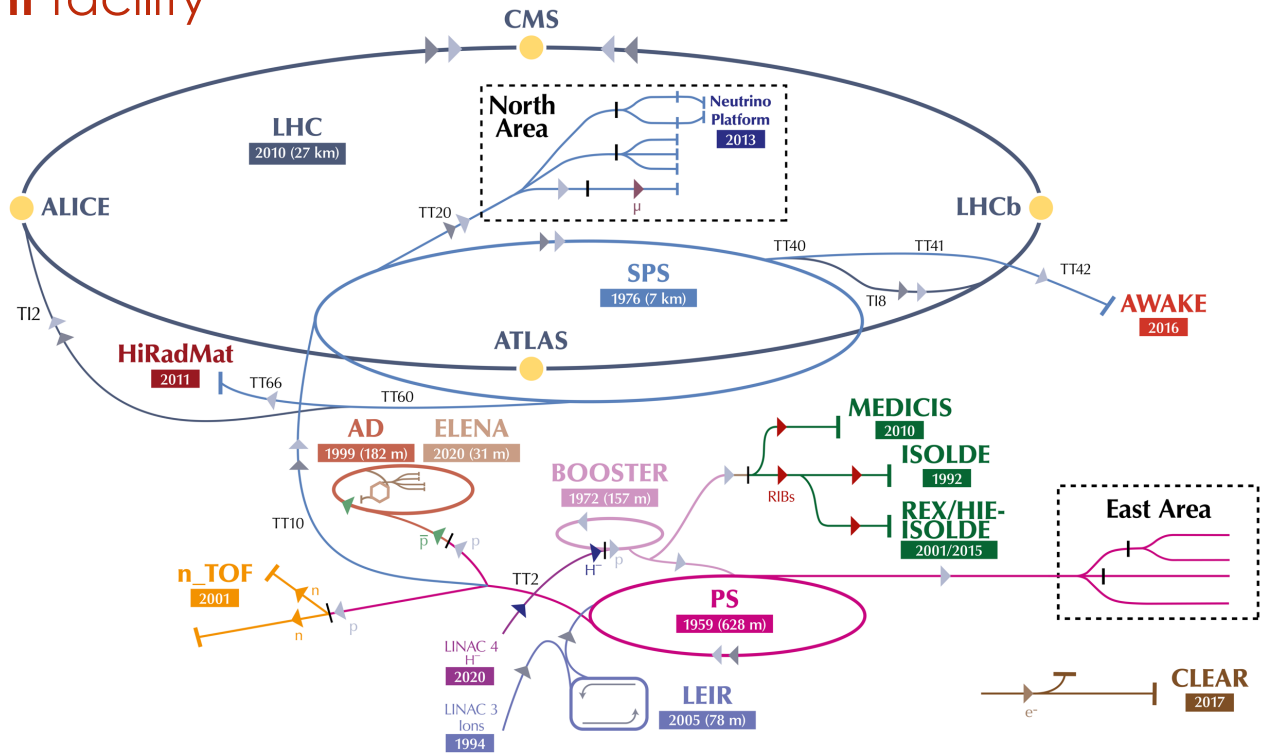
Nuclear Physics in Astrophysics - X

4–9 Sept 2022
CERN



Credit: ESO & ESA/Hubble & NASA

n_TOF: neutron time-of-flight facility @ CERN



▶ H^- (hydrogen anions) ▶ p (protons) ▶ ions ▶ RIBs (Radioactive Ion Beams) ▶ n (neutrons) ▶ \bar{p} (antiprotons) ▶ e^- (electrons) ▶ μ (muons)

LHC - Large Hadron Collider // SPS - Super Proton Synchrotron // PS - Proton Synchrotron // AD - Antiproton Decelerator // CLEAR - CERN Linear Electron Accelerator for Research // AWAKE - Advanced WAKEfield Experiment // ISOLDE - Isotope Separator OnLine // REX/HIE-ISOLDE - Radioactive



NPA-X 2022, 4-9 September 2022, CERN



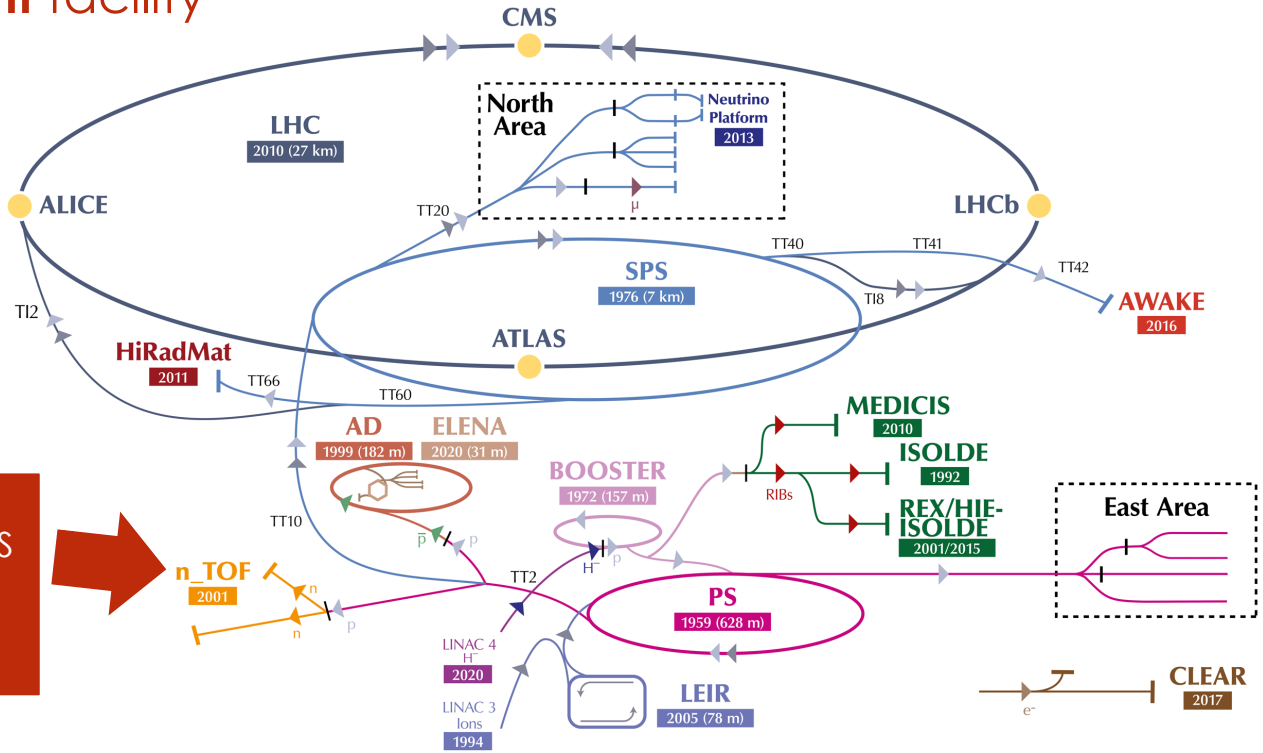
Credit: CERN

massimi@bo.infn.it



ALMA MATER STUDIORUM
UNIVERSITÀ DI BOLOGNA

n_TOF: neutron time-of-flight facility @ CERN



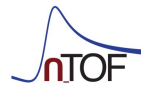
C. Rubbia et al., A high resolution spallation driven facility at the CERN-PS to measure neutron cross sections in the interval from 1 eV to 250 MeV CERN/LHC/98 02(EET) 1998



- ▶ H^- (hydrogen anions)
- ▶ p (protons)
- ▶ ions
- ▶ RIBs (Radioactive Ion Beams)
- ▶ n (neutrons)
- ▶ \bar{p} (antiprotons)
- ▶ e^- (electrons)
- ▶ μ (muons)

LHC - Large Hadron Collider // SPS - Super Proton Synchrotron // PS - Proton Synchrotron // AD - Antiproton Decelerator // CLEAR - CERN Linear Electron Accelerator for Research // AWAKE - Advanced WAKEfield Experiment // ISOLDE - Isotope Separator OnLine // REX/HIE-ISOLDE - Radioactive

NPA-X 2022, 4-9 September 2022, CERN




Credit: CERN

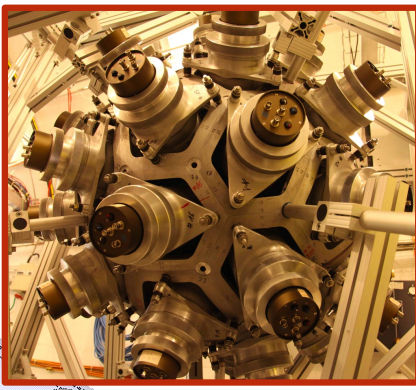
massimi@bo.infn.it



t
i
m
e



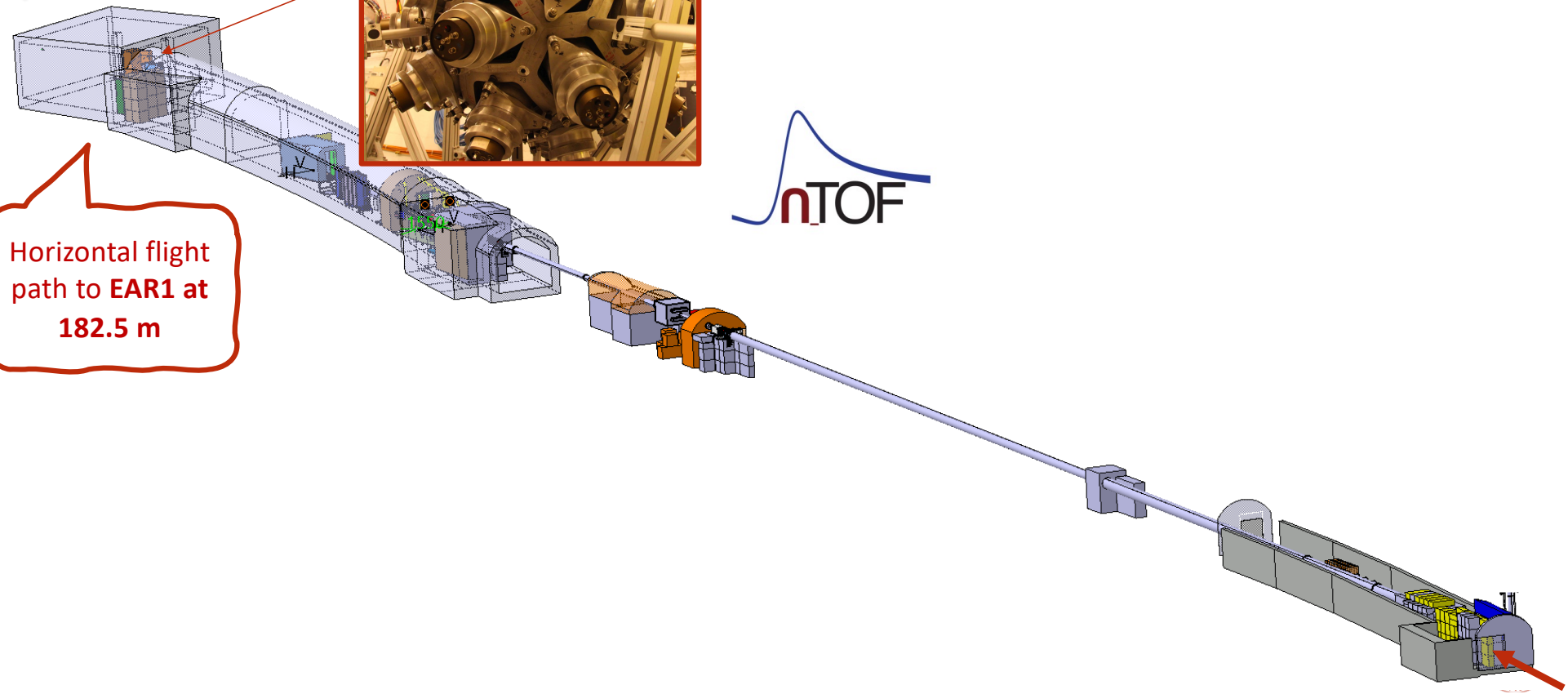
t
i
m
e
↓
EAR1: since 2001



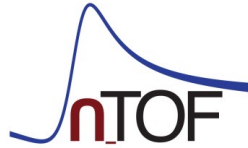
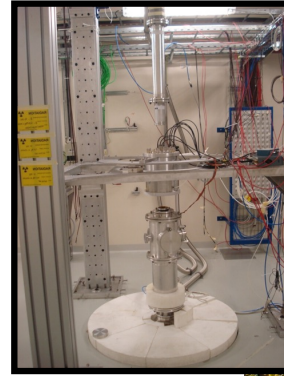
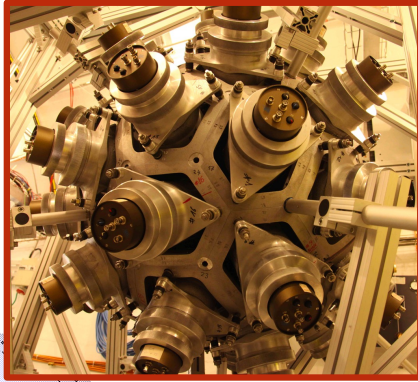
Horizontal flight path to EAR1 at 182.5 m



20 GeV/c protons from the PS

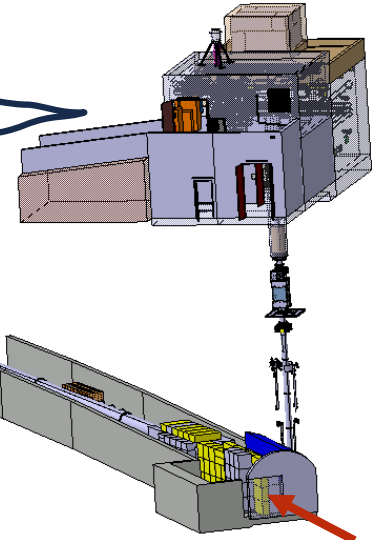


t
i
m
e
↓
EAR1: since 2001
EAR2: since 2014



Horizontal flight path to EAR1 at 182.5 m

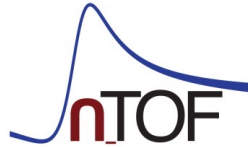
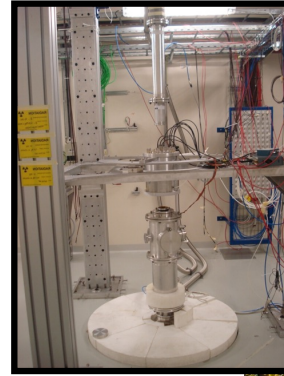
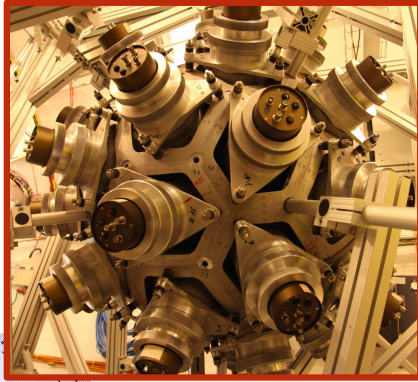
vertical flight path to EAR2 at 19 m



20 GeV/c protons from the PS

t
i
m
e

EAR1: since 2001
EAR2: since 2014
NEAR: Since 2021

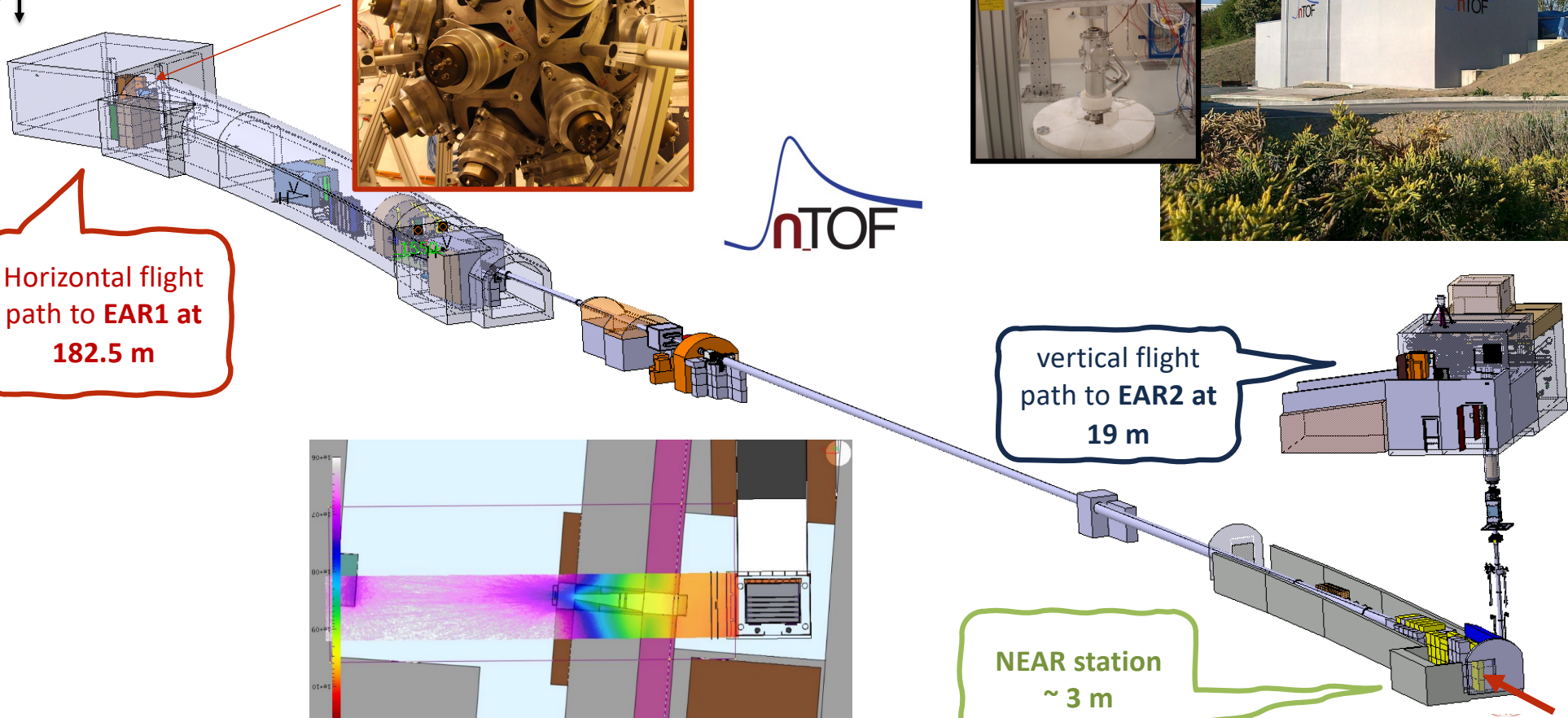
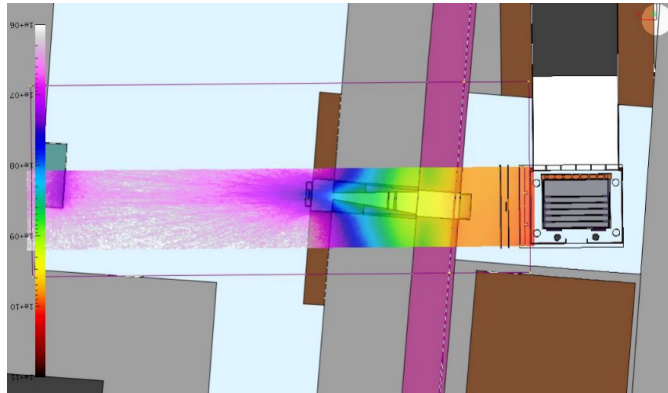


Horizontal flight path to EAR1 at **182.5 m**

vertical flight path to EAR2 at **19 m**

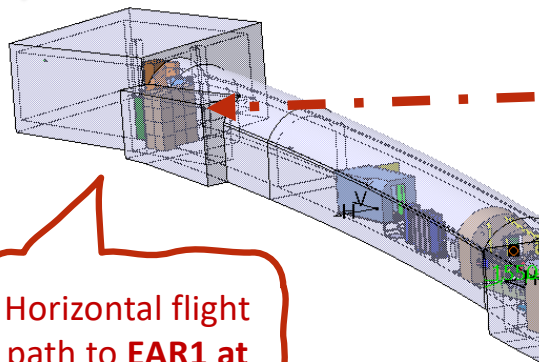
NEAR station **~ 3 m**

20 GeV/c protons from the PS

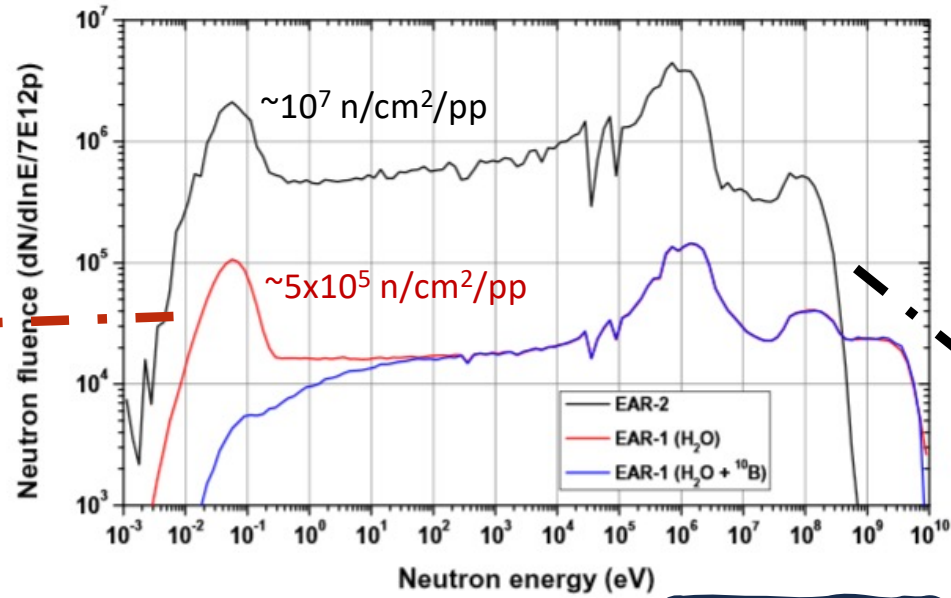


t
i
m
e

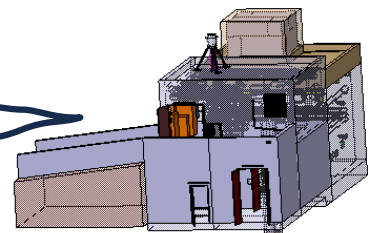
EAR1: since 2001
EAR2: since 2014
NEAR: Since 2021



Horizontal flight path to EAR1 at 182.5 m



vertical flight path to EAR2 at 19 m



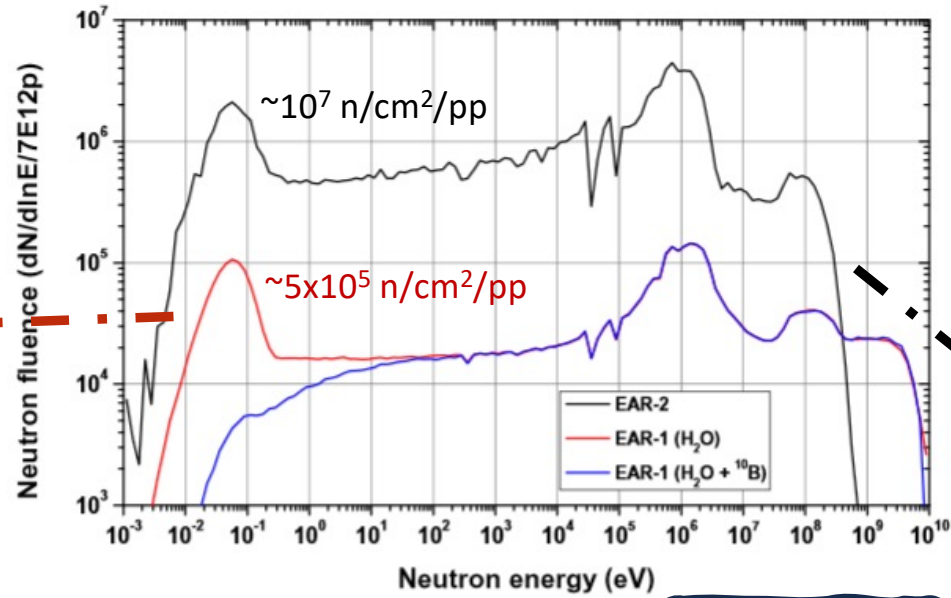
NEAR station ~ 3 m

20 GeV/c protons from the PS

Neutron energy region	n/cm ² /pp
ALL energies	4.6x10 ⁸
E _n <1 keV	0.2x10 ⁸
1 keV<E _n <1 MeV	2.9x10 ⁸
E _n >1 MeV	1.5x10 ⁸

t
i
m
e

EAR1: since 2001
EAR2: since 2014
NEAR: Since 2021



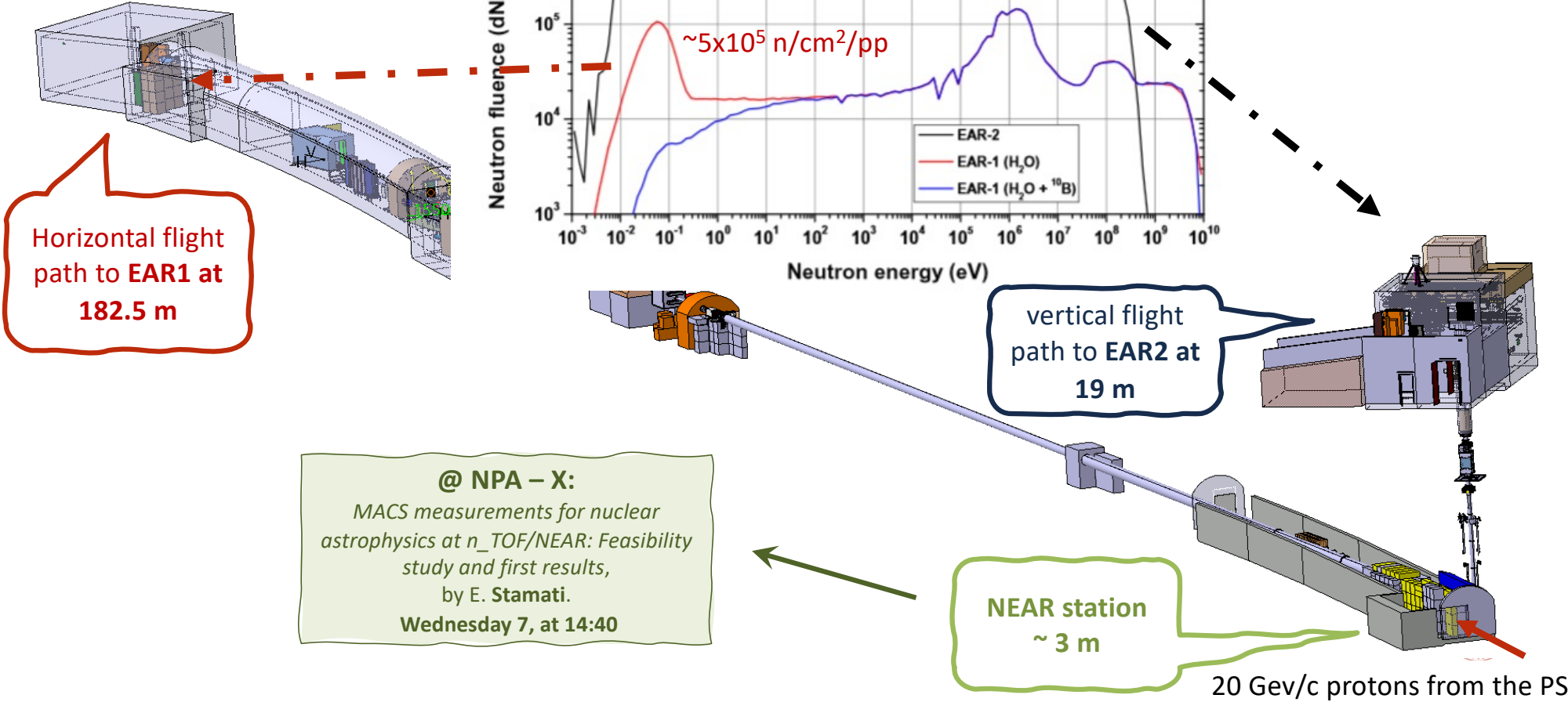
Horizontal flight path to EAR1 at 182.5 m

vertical flight path to EAR2 at 19 m

NEAR station ~ 3 m

@ NPA – X:
MACS measurements for nuclear astrophysics at n_TOF/NEAR: Feasibility study and first results, by E. Stamati. Wednesday 7, at 14:40

20 GeV/c protons from the PS



n_TOF @ CERN

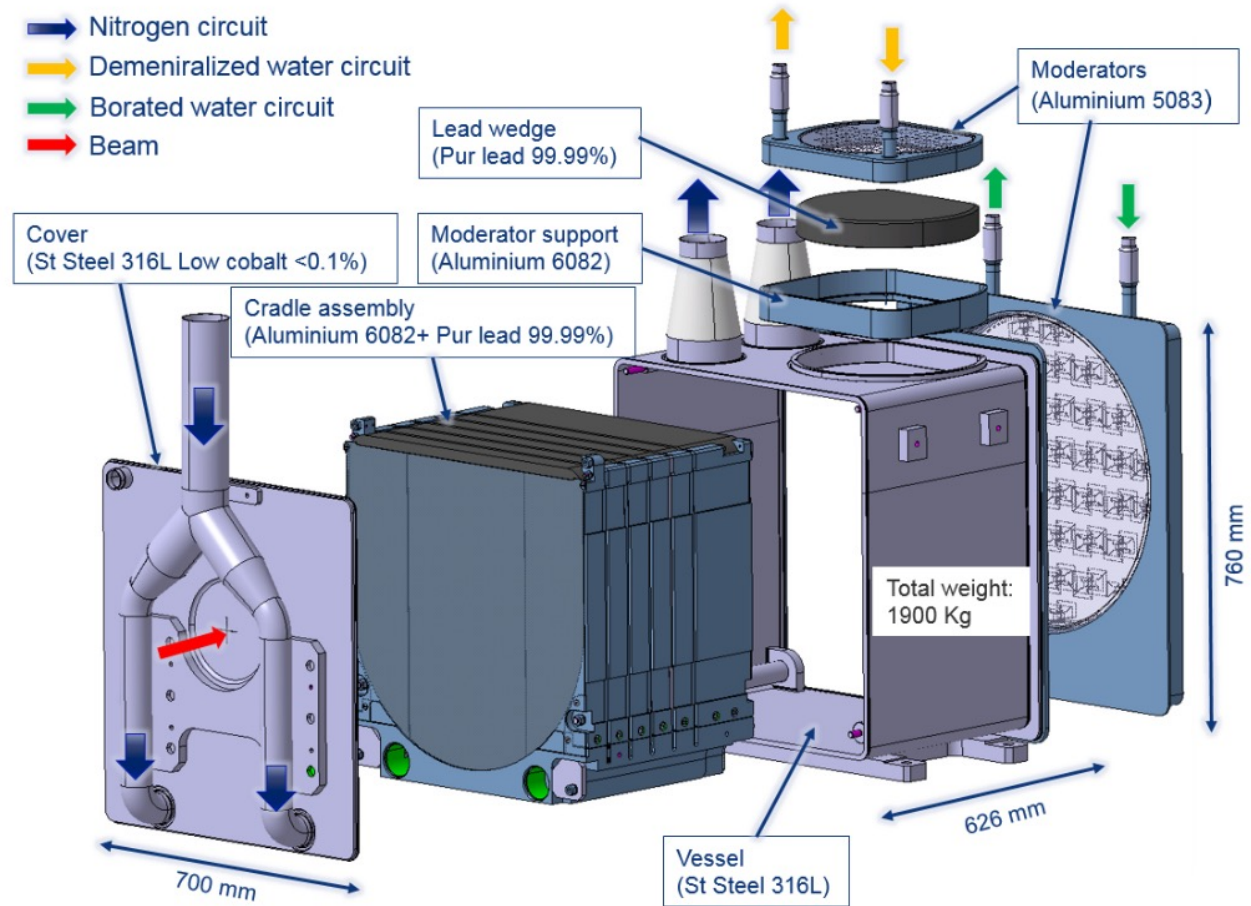
The advantages of n_TOF are a direct consequence of the characteristics of the **PS proton beam**:
high energy, high peak current, low duty cycle.

proton beam momentum	20 GeV/c
intensity (dedicated mode)	7×10^{12} protons/pulse
repetition frequency	1 pulse/1.2s
pulse width	6 ns (rms)
n/p	300
lead target dimensions	$80 \times 80 \times 60 \text{ cm}^3$
cooling & moderation material	N ₂ & H ₂ O (borated)
moderator thickness in the exit face	5 cm
neutron beam dimension in EAR-1 (capture mode)	2 cm (FWHM)

n_TOF @ CERN

3rd generation spallation target

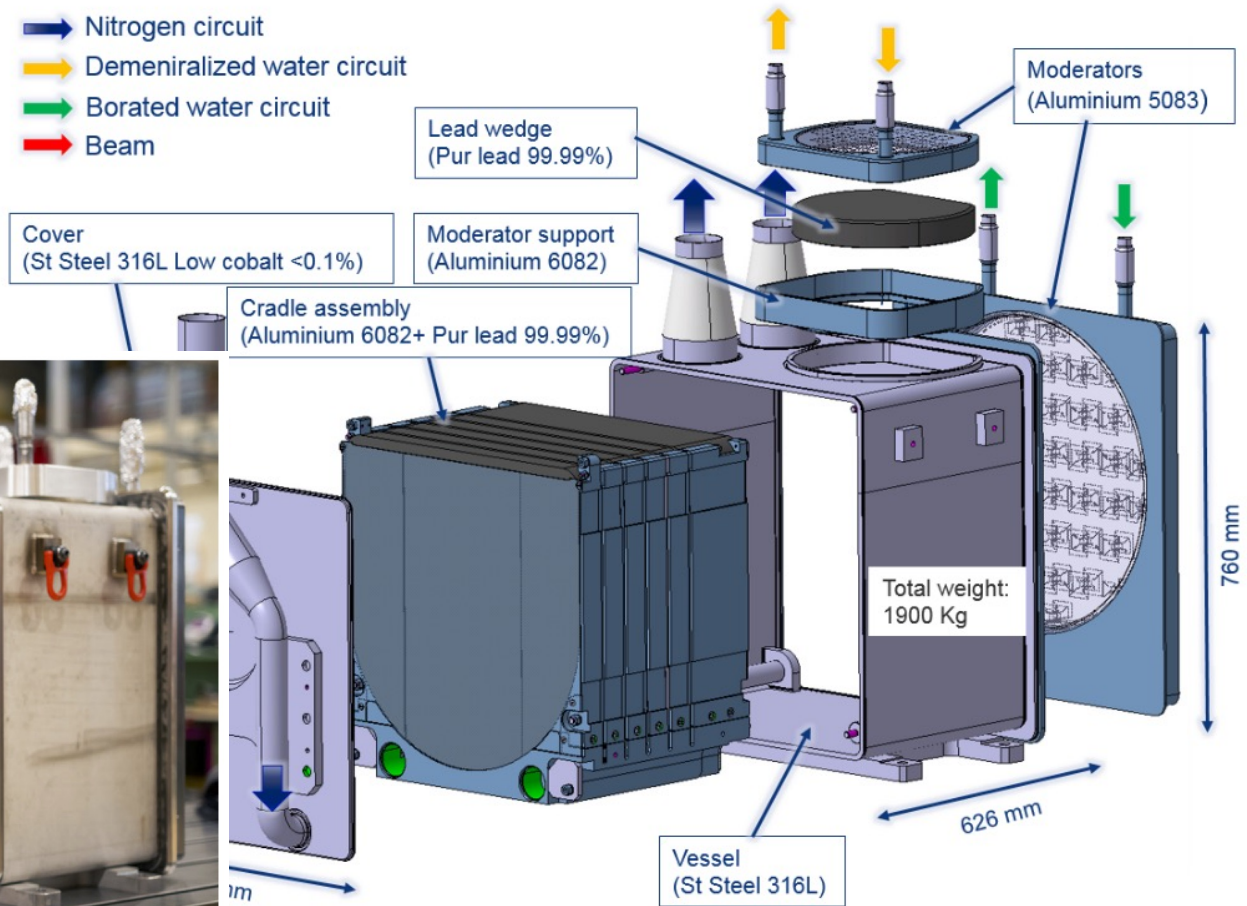
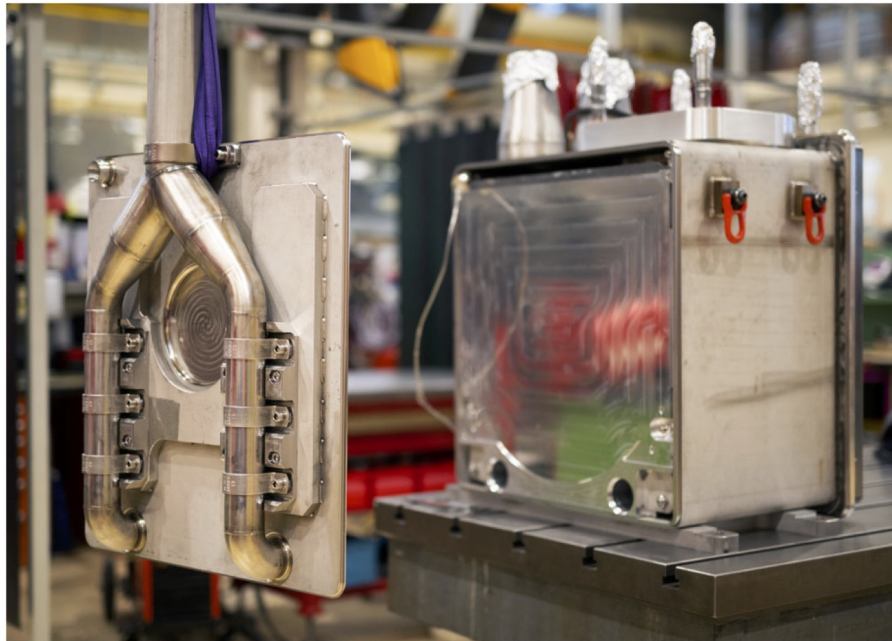
- ❖ pure Pb based
- ❖ N₂-gas cooled, water moderated
- ❖ Several innovations have been introduced



courtesy of Oliver Aberle and Marco Calviani, CERN

n_TOF @ CERN

3rd generation spallation target



courtesy of Oliver Aberle and Marco Calviani, CERN



NPA-X 2022, 4-9 September 2022, CERN

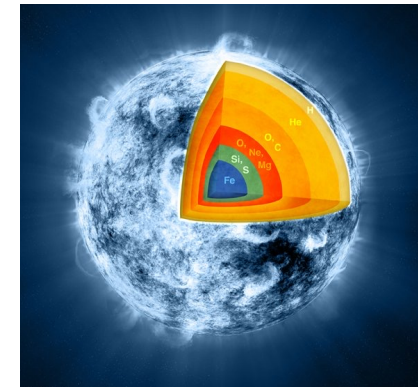
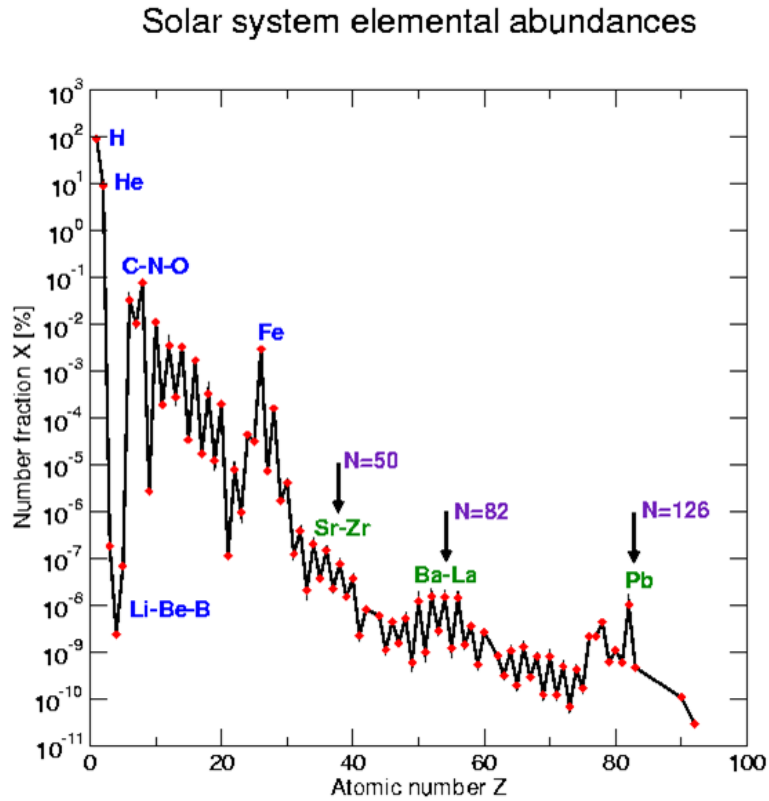
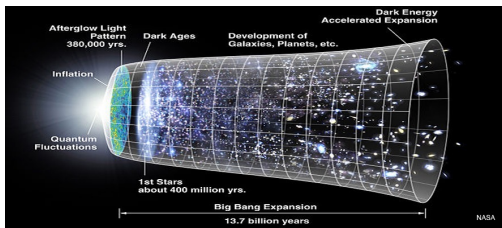


massimi@bo.infn.it



n_TOF: nuclear data for science (and technology)

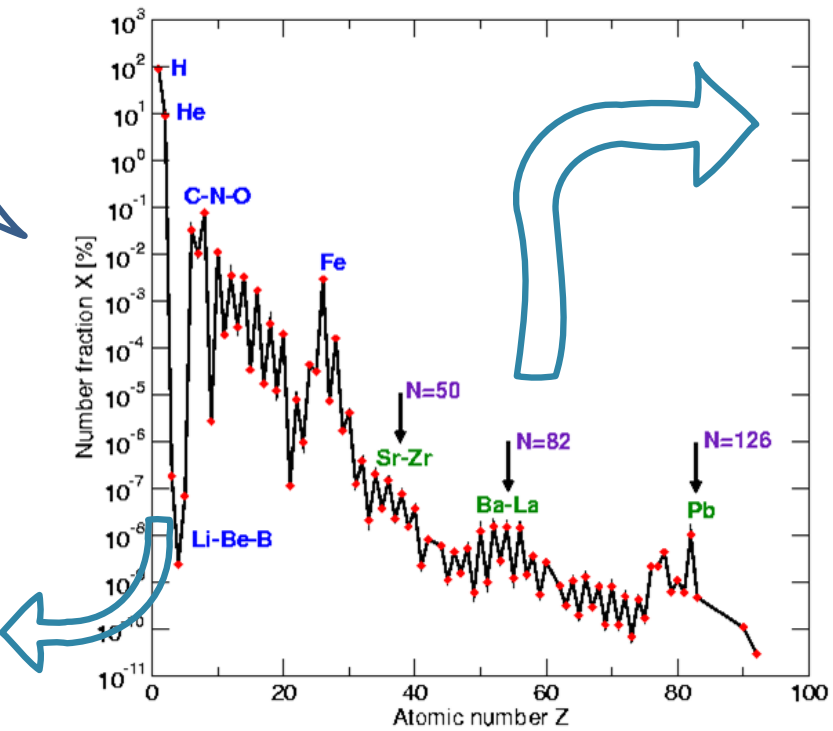
How chemical elements are synthesized in the Universe?



n_TOF: nuclear data for science (and technology) @ NPA - X

Solar system elemental abundances

How chemical elements are synthesized in the Universe?



BIG BANG Nucleosynthesis:

- ${}^7\text{Be}(n, \alpha)$ and ${}^7\text{Be}(n, p)$ cross section measurement for the Cosmological Lithium Problem.

Later in this presentation

s process:

- first measurement of the ${}^{94}\text{Nb}$ neutron capture cross-section at the cern n_TOF facility, by J. Balibrea Correa. **Tuesday 6, at 9:30**
- MACS measurements for nuclear astrophysics at n_TOF/NEAR: Feasibility study and first results, by E. Stamati. **Wednesday 7, at 14:40**
- New detection systems for an enhanced sensitivity in key stellar (n, γ) measurements, by J. Lerendegui Marco. **Thursday 8, at 11:00**
- Measurement of the ${}^{140}\text{Ce}(n, \gamma)$ cross section at n_TOF and astrophysical implications, by S. Amaducci. **Thursday 8, at 11:30**
- Poster by S. Lanzi: The impact of n_TOF data on s-process nucleosynthesis

n_TOF: nuclear data for science (and technology) @ NPA - X

How chemical elements are synthesized in the Universe?

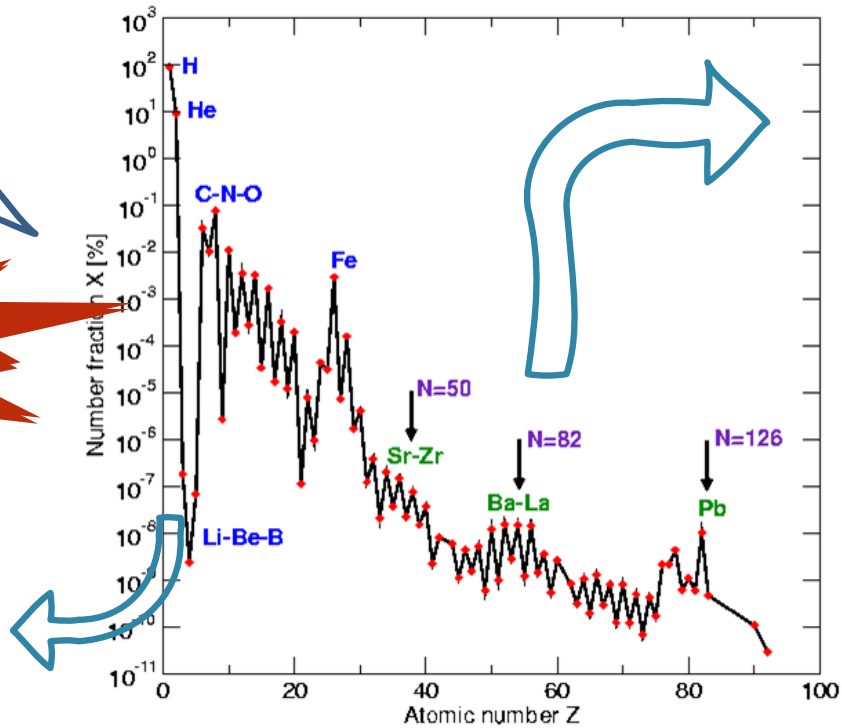
Poster by G. Gervino:
X17 search project with the EAR2 neutron beam

BIG BANG Nucleosynthesis:

- ${}^7\text{Be}(n, \alpha)$ and ${}^7\text{Be}(n, p)$ cross section measurement for the Cosmological Lithium Problem.

Later in this presentation

Solar system elemental abundances



s process:

- first measurement of the ${}^{94}\text{Nb}$ neutron capture cross-section at the cern n_TOF facility, by J. Balibrea Correa. **Tuesday 6, at 9:30**
- MACS measurements for nuclear astrophysics at n_TOF/NEAR: Feasibility study and first results, by E. Stamati. **Wednesday 7, at 14:40**
- New detection systems for an enhanced sensitivity in key stellar (n, γ) measurements, by J. Lerendegui Marco. **Thursday 8, at 11:00**
- Measurement of the ${}^{140}\text{Ce}(n, \gamma)$ cross section at n_TOF and astrophysical implications, by S. Amaducci. **Thursday 8, at 11:30**
- Poster by S. Lanzi: The impact of n_TOF data on s-process nucleosynthesis

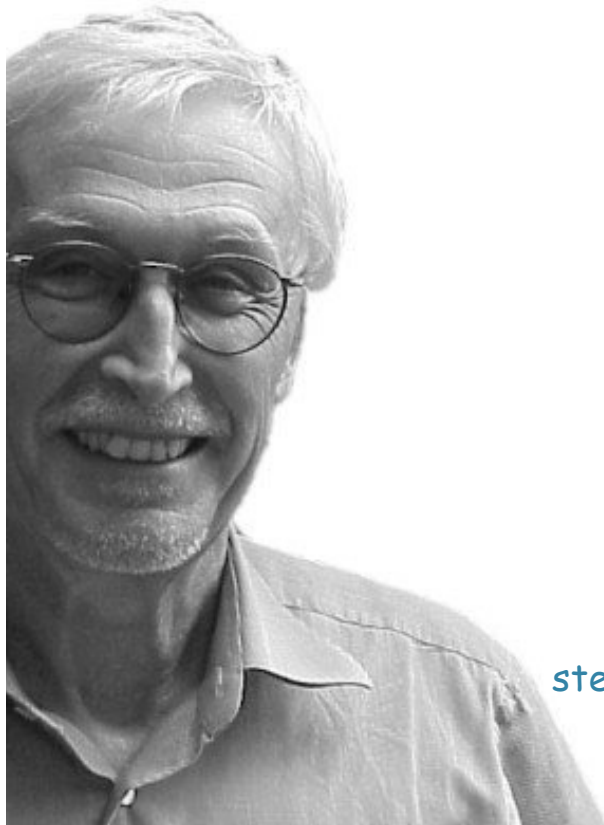
n_TOF: nuclear data for science (and technology) ... so far

Radiative capture reactions (n, γ)	(89)
Fission reactions (n,f)	(37)
Light particle emission reactions (n,lcp)	(11)
Detector developments	(6)

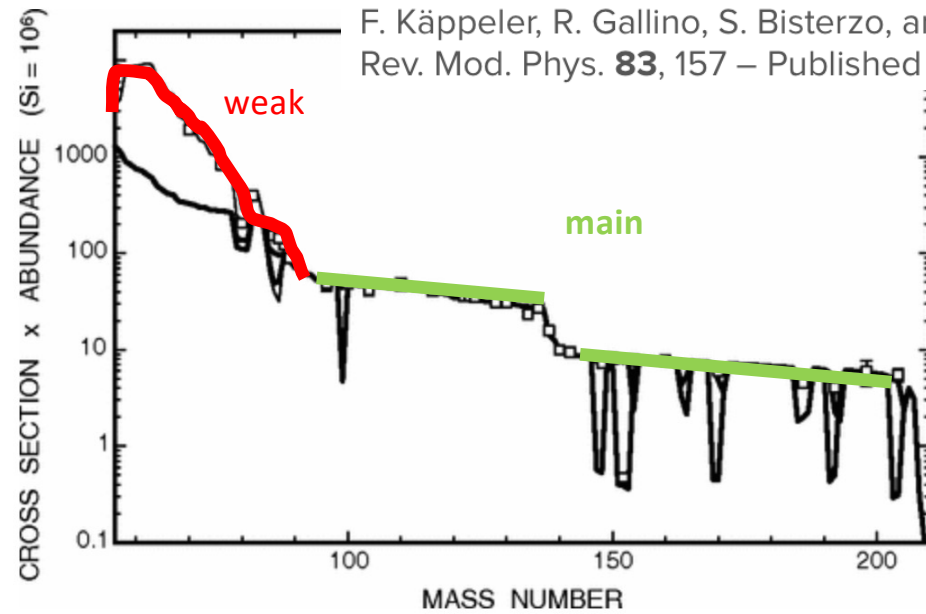
The n_TOF Collaboration list of publications:
<https://twiki.cern.ch/NTOFPublic/ListOfPublications>



Stellar cross sections (MACS) for the s process



MACS
or
stellar cross section



F. Käppeler, R. Gallino, S. Bisterzo, and Wako Aoki
Rev. Mod. Phys. **83**, 157 – Published 1 April 2011

weak: core He burning in massive stars

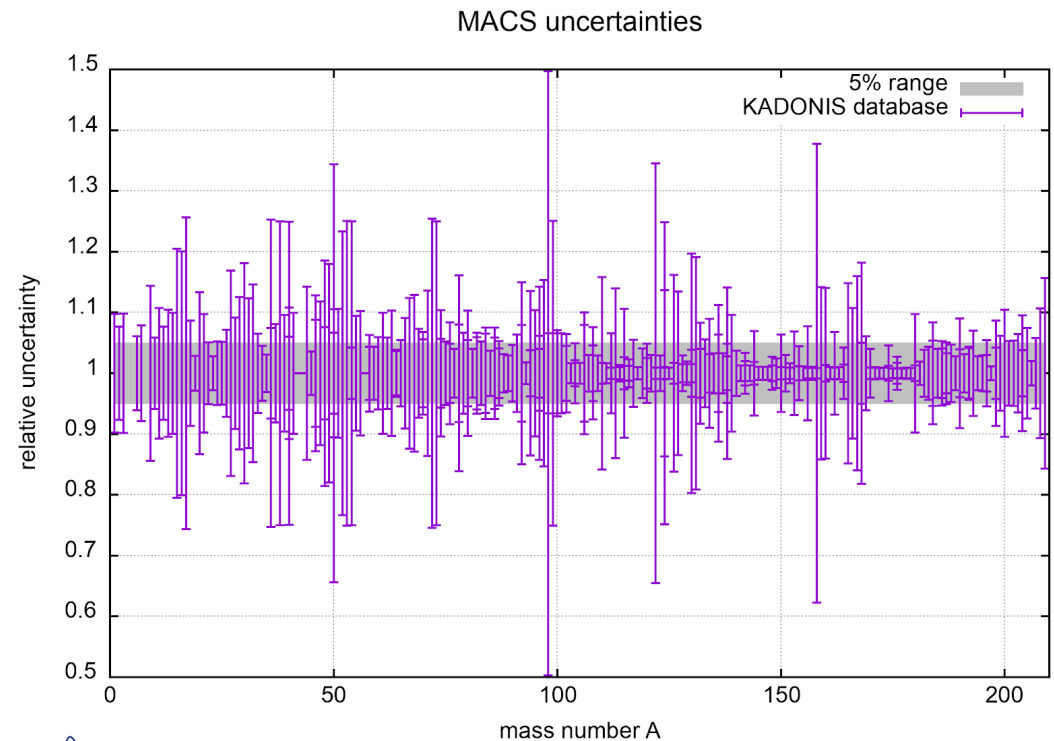
main: He shell flashes in low mass TP-AGB stars

Stellar cross sections (MACS) for the s process

F. Käppeler, R. Gallino, S. Bisterzo, and Wako Aoki
Rev. Mod. Phys. **83**, 157 – Published 1 April 2011

Reducing the uncertainty in the stellar cross section (MACS) is not only a question of better nuclear data: **higher accuracy** in the **reaction rates** opens the possibility to **investigate new astrophysical scenarios**

[nuclear clocks, constrains on the BBN, AGB modelling, nucleosynthesis conditions in explosive scenarios, meteoritic grains, others]

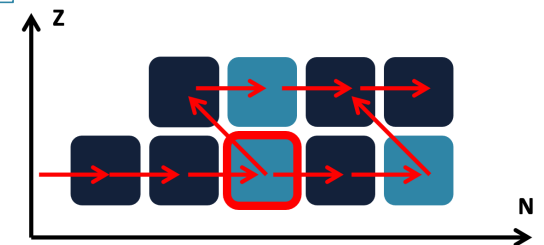


Stellar cross sections (MACS) for the s process

U. Abbondanno, et al. (The n_TOF Collaboration), [Phys. Rev. Lett. 94 \(2004\) 161103](#)
 C. Lederer, et al. (The n_TOF Collaboration), [Phys. Rev. Lett 110 \(2013\) 022501](#)
 C. Guerrero, et al. (The n_TOF Collaboration), [Phys. Rev. Lett. 125 \(2020\) 142701](#)

F. Käppeler, R. Gallino, S. Bisterzo, and Wako Aoki
 Rev. Mod. Phys. **83**, 157 – Published 1 April 2011

Sample	Half-life (yr)	Q value (MeV)	Comment
⁶³ Ni	100.1	β^- , 0.066	TOF work in progress (Couture, 2009), sample with low enrichment
⁷⁹ Se	2.95×10^5	β^- , 0.159	Important branching, constrains s-process temperature in massive stars
⁸¹ Kr	2.29×10^5	EC, 0.322	Part of ⁷⁹ Se branching
⁸⁵ Kr	10.73	β^- , 0.687	Important branching, constrains neutron density in massive stars
⁹⁵ Zr	64.02 d	β^- , 1.125	Not feasible in near future, but important for neutron density low-mass AGB stars
¹³⁴ Cs	2.0652	β^- , 2.059	Important branching at A = 134, 135, sensitive to s-process temperature in low-mass AGB stars, measurement not feasible in near future
¹³⁵ Cs	2.3×10^6	β^- , 0.269	So far only activation measurement at kT = 25 keV by Patronis <i>et al.</i> (2004)
¹⁴⁷ Nd	10.981 d	β^- , 0.896	Important branching at A = 147/148, constrains neutron density in low-mass AGB stars
¹⁴⁷ Pm	2.6234	β^- , 0.225	Part of branching at A = 147/148
¹⁴⁸ Pm	5.368 d	β^- , 2.464	Not feasible in the near future
¹⁵¹ Sm	90	β^- , 0.076	Existing TOF measurements, full set of MACS data available (Abbondanno <i>et al.</i> , 2004a; Wisshak <i>et al.</i> , 2006c)
¹⁵⁴ Eu	8.593	β^- , 1.978	Complex branching at A = 154, 155, sensitive to temperature and neutron density
¹⁵⁵ Eu	4.753	β^- , 0.246	So far only activation measurement at kT = 25 keV by Jaag and Käppeler (1995)
¹⁵³ Gd	0.658	EC, 0.244	Part of branching at A = 154, 155
¹⁶⁰ Tb	0.198	β^- , 1.833	Weak temperature-sensitive branching, very challenging experiment
¹⁶³ Ho	4570	EC, 0.0026	Branching at A = 163 sensitive to mass density during s process, so far only activation measurement at kT = 25 keV by Jaag and Käppeler (1996b)
¹⁷⁰ Tm	0.352	β^- , 0.968	Important branching, constrains neutron density in low-mass AGB stars
¹⁷¹ Tm	1.921	β^- , 0.098	Part of branching at A = 170, 171
¹⁷⁹ Ta	1.82	EC, 0.115	Crucial for s-process contribution to ¹⁸⁰ Ta, nature's rarest stable isotope
¹⁸⁵ W	0.206	β^- , 0.432	Important branching, sensitive to neutron density and s-process temperature in low-mass AGB stars
²⁰⁴ Tl	3.78	β^- , 0.763	Determines ²⁰⁵ Pb/ ²⁰⁵ Tl clock for dating of early Solar System



Stellar cross sections (MACS) for the s process

U. Abbondanno, et al. (The n_TOF Collaboration), [Phys. Rev. Lett. 94 \(2004\) 161103](#)
 C. Lederer, et al. (The n_TOF Collaboration), [Phys. Rev. Lett 110 \(2013\) 022501](#)
 C. Guerrero, et al. (The n_TOF Collaboration), [Phys. Rev. Lett. 125 \(2020\) 142701](#)

F. Käppeler, R. Gallino, S. Bisterzo, and Wako Aoki
 Rev. Mod. Phys. **83**, 157 – Published 1 April 2011

Sample	Half-life (yr)	Q value (MeV)	Comment
⁶³ Ni	100.1	β^- , 0.066	TOF work in progress (Couture, 2009), sample with low enrichment
⁷⁹ Se	2.95×10^5	β^- , 0.159	Important branching, constrains s-process temperature in massive stars
⁸¹ Kr	2.29×10^7	EC, 0.322	Part of ⁷⁹ Se branching
⁸⁵ Kr	10.73	β^- , 0.687	Important branching, constrains neutron density in massive stars
⁹⁵ Zr	64.02 d	β^- , 1.125	Not feasible in near future, but important for neutron density low-mass AGB stars
¹³⁴ Cs	2.0652	β^- , 2.059	Important branching at A = 134, 135, sensitive to s-process temperature in low-mass AGB stars, measurement not feasible in near future
¹³⁵ Cs	2.3×10^6	β^- , 0.269	So far only activation measurement at kT = 25 keV by Patronis <i>et al.</i> (2004)
¹⁴⁷ Nd	10.981 d	β^- , 0.896	Important branching at A = 147/148, constrains neutron density in low-mass AGB stars
¹⁴⁷ Pm	2.6234	β^- , 0.225	Part of branching at A = 147/148
¹⁴⁸ Pm	5.368 d	β^- , 2.464	Not feasible in the near future
¹⁵¹ Sm	90	β^- , 0.076	Existing TOF measurements, full set of MACS data available (Abbondanno <i>et al.</i> , 2004a; Wisshak <i>et al.</i> , 2006c)
¹⁵⁴ Eu	8.593	β^- , 1.978	Complex branching at A = 154, 155, sensitive to temperature and neutron density
¹⁵⁵ Eu	4.753	β^- , 0.246	So far only activation measurement at kT = 25 keV by Jaag and Käppeler (1995)
¹⁵³ Gd	0.658	EC, 0.244	Part of branching at A = 154, 155
¹⁶⁰ Tb	0.198	β^- , 1.833	Weak temperature-sensitive branching, very challenging experiment
¹⁶³ Ho	4570	EC, 0.0026	Branching at A = 163 sensitive to mass density during s process, so far only activation measurement at kT = 25 keV by Jaag and Käppeler (1996b)
¹⁷⁰ Tm	0.352	β^- , 0.968	Important branching, constrains neutron density in low-mass AGB stars
¹⁷¹ Tm	1.921	β^- , 0.098	Part of branching at A = 170, 171
¹⁷⁹ Ta	1.82	EC, 0.115	Crucial for s-process contribution to ¹⁸⁰ Ta, nature's rarest stable isotope
¹⁸⁵ W	0.206	β^- , 0.432	Important branching, sensitive to neutron density and s-process temperature in low-mass AGB stars
²⁰⁴ Tl	3.78	β^- , 0.763	Determines ²⁰⁵ Pb/ ²⁰⁵ Tl clock for dating of early Solar System



European Research Council

@ NPA – X:

New detection systems for an enhanced sensitivity in key stellar (n, γ) measurements,

by J. Lereendgui Marco.

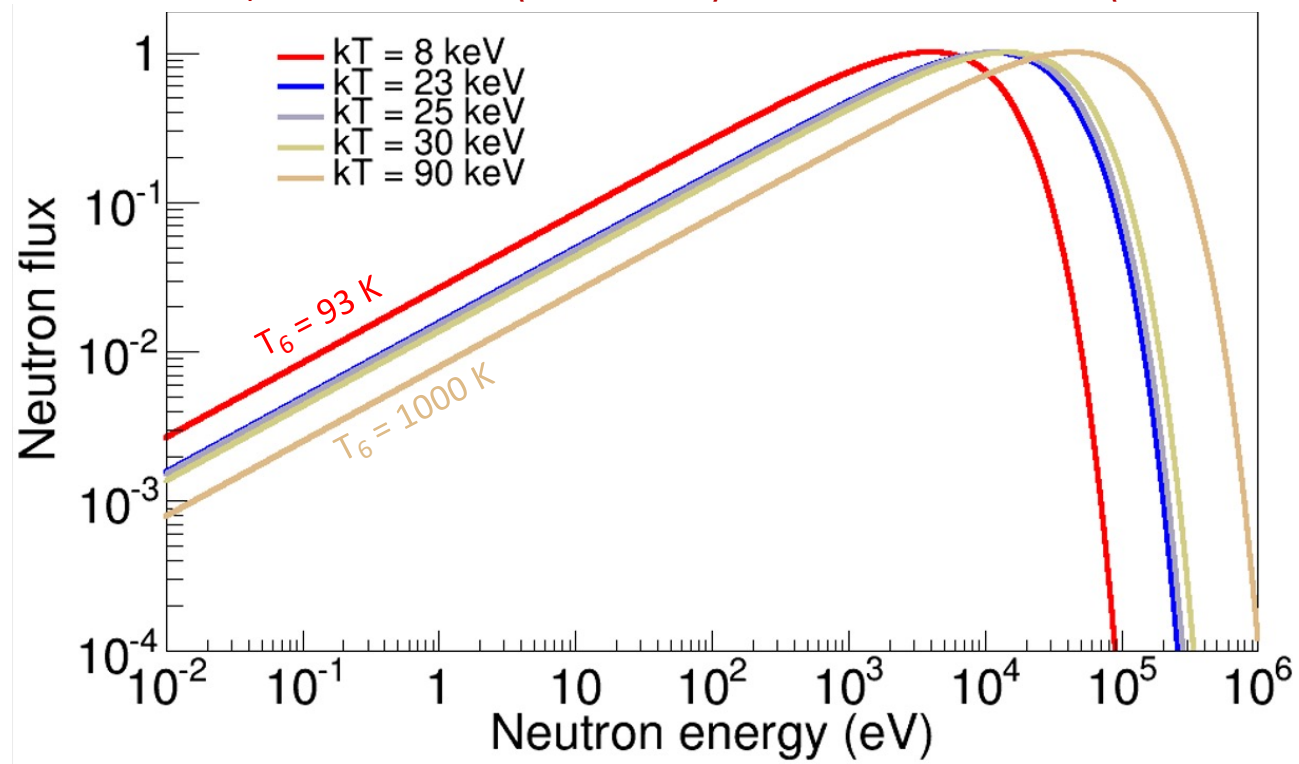
Thursday 8, at 11:00



ALMA MATER STUDIORUM
UNIVERSITÀ DI BOLOGNA

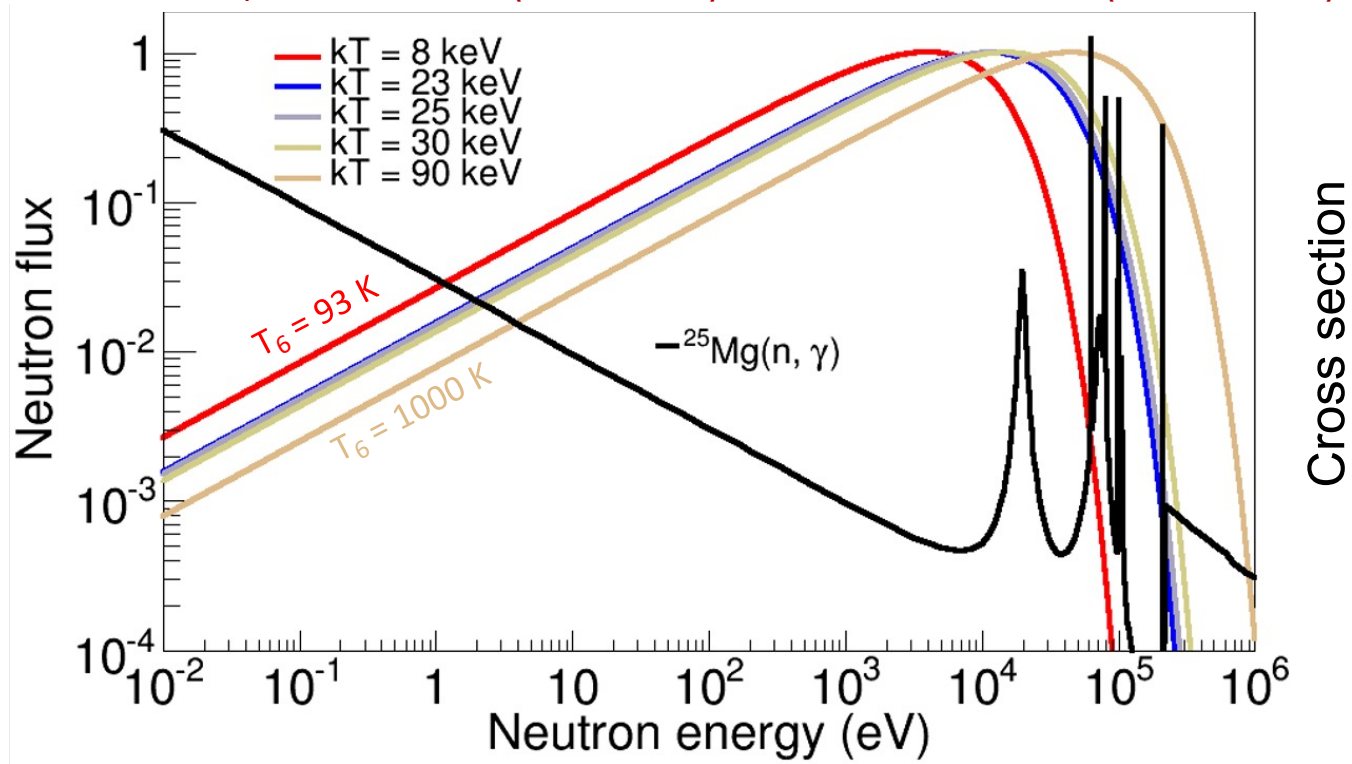
Stellar cross sections (MACS) for the s process

Stellar spectra: AGB (8, 23 keV) and Massive stars (25, 90 keV)

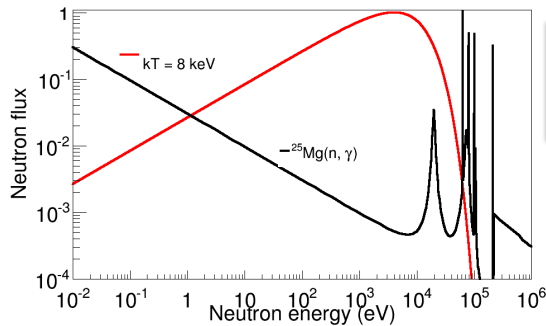


Stellar cross sections (MACS) for the s process

Stellar spectra: AGB (8, 23 keV) and Massive stars (25, 90 keV)



Stellar cross sections (MACS) for the s process



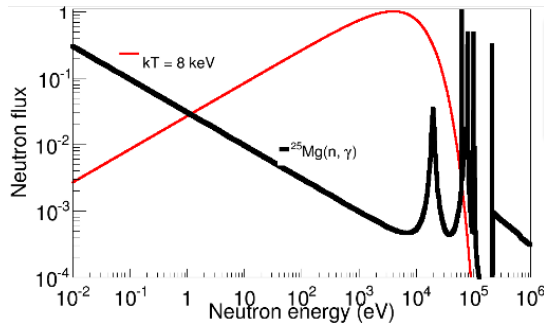
What is important is the **Maxwellian Averaged Cross-Sections (MACS)** at various **temperatures** (kT depends on stellar site).

Reaction rate ($\text{cm}^{-3}\text{s}^{-1}$): $r = N_A N_n v \sigma(v) \longrightarrow r = N_A N_n \langle \sigma \cdot v \rangle$

$$\text{MACS} \equiv \frac{\langle \sigma \cdot v \rangle}{v_T} = \frac{2}{\sqrt{\pi}(kT)^2} \int_0^\infty \sigma(E) E e^{-E/(kT)} dE$$

Two methods to determine MACS:

Stellar cross sections (MACS) for the s process

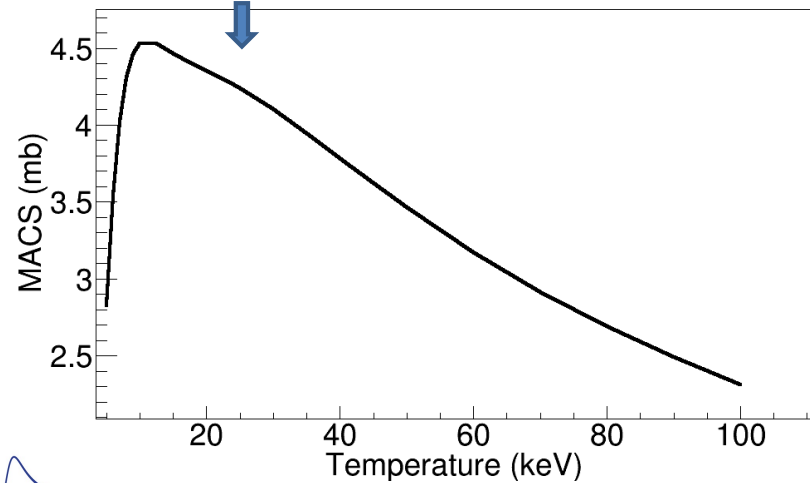


What is important is the **Maxwellian Averaged Cross-Sections (MACS)** at various **temperatures** (kT depends on stellar site).

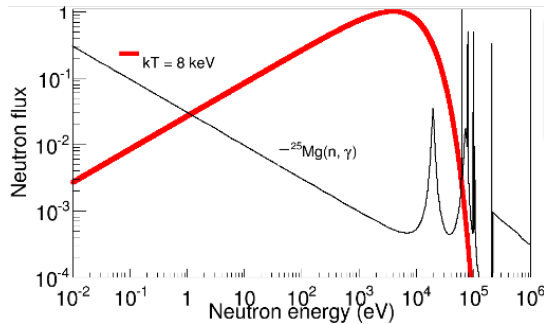
Reaction rate (cm⁻³s⁻¹): $r = N_A N_n v \sigma(v) \rightarrow r = N_A N_n \langle \sigma \cdot v \rangle$

$$MACS \equiv \frac{\langle \sigma \cdot v \rangle}{v_T} = \frac{2}{\sqrt{\pi}(kT)^2} \int_0^\infty \sigma(E) E e^{-E/(kT)} dE$$

- Two methods to determine MACS:**
1. measurement of **energy dependent** neutron capture cross-sections → EAR1 & EAR2



Stellar cross sections (MACS) for the s process

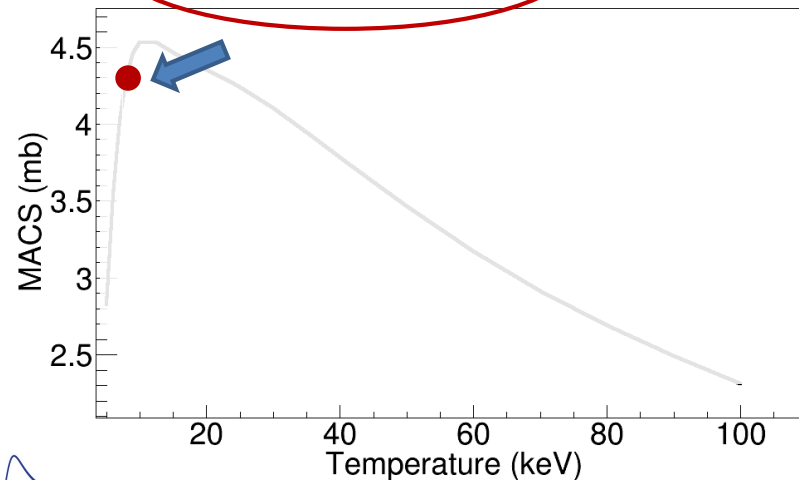


What is important is the **Maxwellian Averaged Cross-Sections (MACS)** at various **temperatures** (kT depends on stellar site).

Reaction rate (cm⁻³s⁻¹): $r = N_A N_n v \sigma(v) \Rightarrow r = N_A N_n \langle \sigma \cdot v \rangle$

$$MACS \equiv \frac{\langle \sigma \cdot v \rangle}{v_T} = \frac{2}{\sqrt{\pi}(kT)^2} \int_0^\infty \sigma(E) E e^{-E/(kT)} dE$$

- Two methods to determine MACS:**
1. measurement of **energy dependent** neutron capture cross-sections → **EAR1 & EAR2**
 2. **integral measurement** (energy integrated) using neutron beams with suitable energy → **NEAR**



Stellar cross sections (MACS) for the s process

Fission program not included in the list !!!

Cross sections measured in 2001 - 2022

- ❖ Branching point isotopes:

^{151}Sm , ^{63}Ni , ^{147}Pm , ^{171}Tm , ^{203}Tl , ^{79}Se

- ❖ Abundances in presolar grains:

$^{91,92,93,94,96}\text{Zr}$, $^{94,96}\text{Mo}$

- ❖ Magic Nuclei and end-point:

^{139}La , ^{140}Ce , ^{90}Zr , ^{89}Y , ^{88}Sr , $^{204,206,207,208}\text{Pb}$, ^{209}Bi

- ❖ Seeds isotopes:

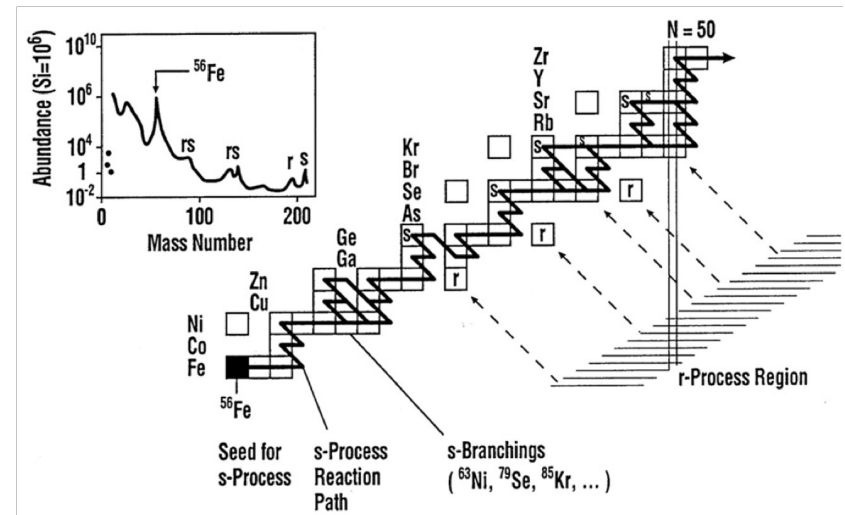
$^{54,56,57}\text{Fe}$, $^{58,60,62}\text{Ni}$, $^{59}\text{Ni}(n,\alpha)$

- ❖ Isotopes of special interest:

$^{186,187,188}\text{Os}$ (cosmochronometer), ^{197}Au (reference cross section), $^{24,25,26}\text{Mg}$, $^{33}\text{S}(n,\alpha)$, $^{14}\text{N}(n,p)$, $^{35}\text{Cl}(n,p)$, $^{26}\text{Al}(n,p)$, $^{26}\text{Al}(n,\alpha)$ (neutron poison), ^{154}Gd (s-only isotopes), $^{93,94}\text{Nb}$, ^{68}Zn , $^{69,71}\text{Ga}$, $^{70,72,73,74,76}\text{Ge}$, $^{77,78,80}\text{Se}$ (weak component), $^{155,157,160}\text{Gd}$, $^7\text{Li}(n,p)$, $^7\text{Li}(n,\alpha)$ **Big Bang Nucleosynthesis**

- ❖ Neutron Sources $^{22}\text{Ne}(\alpha,n)^{25}\text{Mg}$ and $^{13}\text{C}(\alpha,n)^{16}\text{O}$:

$n+^{25}\text{Mg}$, $n+^{16}\text{O}$



Stellar cross sections (MACS) for the s process

Fission program not included in the list !!!

Cross sections measured in 2001 - 2022

- ❖ Branching point isotopes:

^{151}Sm , ^{63}Ni , ^{147}Pm , ^{171}Tm , ^{203}Tl , ^{79}Se

- ❖ Abundances in presolar grains:

$^{91,92,93,94,96}\text{Zr}$, $^{94,96}\text{Mo}$

- ❖ Magic Nuclei and end point:

^{139}La , ^{140}Ce , ^{90}Zr , ^{89}Y , ^{88}Sr

- ❖ Seeds isotopes:

$^{54,56,57}\text{Fe}$, $^{58,60,62}\text{Ni}$, ^{59}Ni

- ❖ Isotopes of special interest:

$^{186,187,188}\text{Os}$ (cosmochronometer), ^{197}Au (reference cross section), $^{24,25,26}\text{Mg}$, $^{33}\text{S}(n,\alpha)$, $^{14}\text{N}(n,p)$, $^{35}\text{Cl}(n,p)$, $^{26}\text{Al}(n,p)$, $^{26}\text{Al}(n,\alpha)$ (neutron poison), ^{154}Gd (s-only isotopes), $^{93,94}\text{Nb}$, ^{68}Zn , $^{69,71}\text{Ga}$, $^{70,72,73,74,76}\text{Ge}$, $^{77,78,80}\text{Se}$ (weak component), $^{155,157,160}\text{Gd}$, $^7\text{Li}(n,p)$, $^7\text{Li}(n,\alpha)$ Big Bang Nucleosynthesis

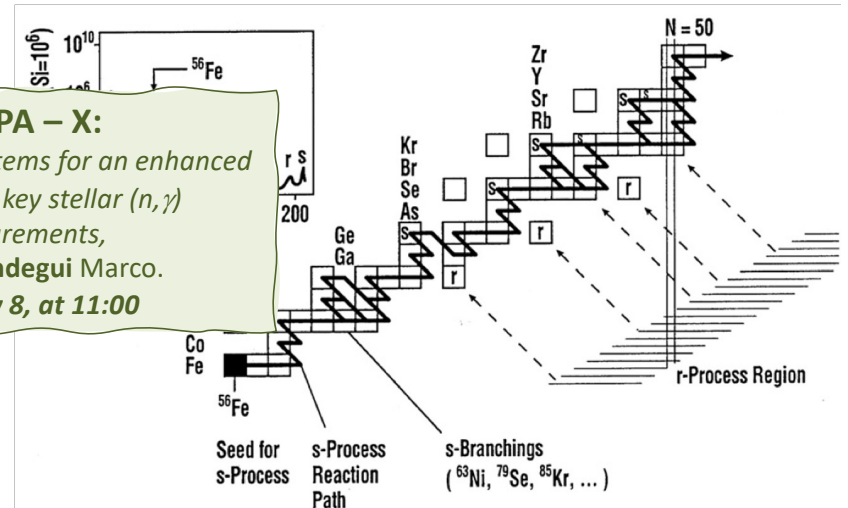
- ❖ Neutron Sources $^{22}\text{Ne}(\alpha,n)^{25}\text{Mg}$ and $^{13}\text{C}(\alpha,n)^{16}\text{O}$:

$n+^{25}\text{Mg}$, $n+^{16}\text{O}$

@ NPA - X:
New detection systems for an enhanced sensitivity in key stellar (n,γ) measurements,
by J. Lerendegui Marco.
Thursday 8, at 11:00

@ NPA - X:
Measurement of the $^{140}\text{Ce}(n,\gamma)$ cross section at n_TOF and astrophysical implications,
by S. Amaducci.
Thursday 8, at 11:30

@ NPA - X:
first measurement of the ^{94}Nb neutron capture cross-section at the cern n_TOF facility,
by J. Balibrea Correa.
Tuesday 6, at 9:30



Examples of relevant and/or challenging measurements

❖ $^{197}\text{Au}(n,\gamma)$

❖ $^7\text{Be}(n,p)$ & $^7\text{Be}(n,\alpha)$

❖ $^{26}\text{Al}(n,p)$ & $^{26}\text{Al}(n,\alpha)$

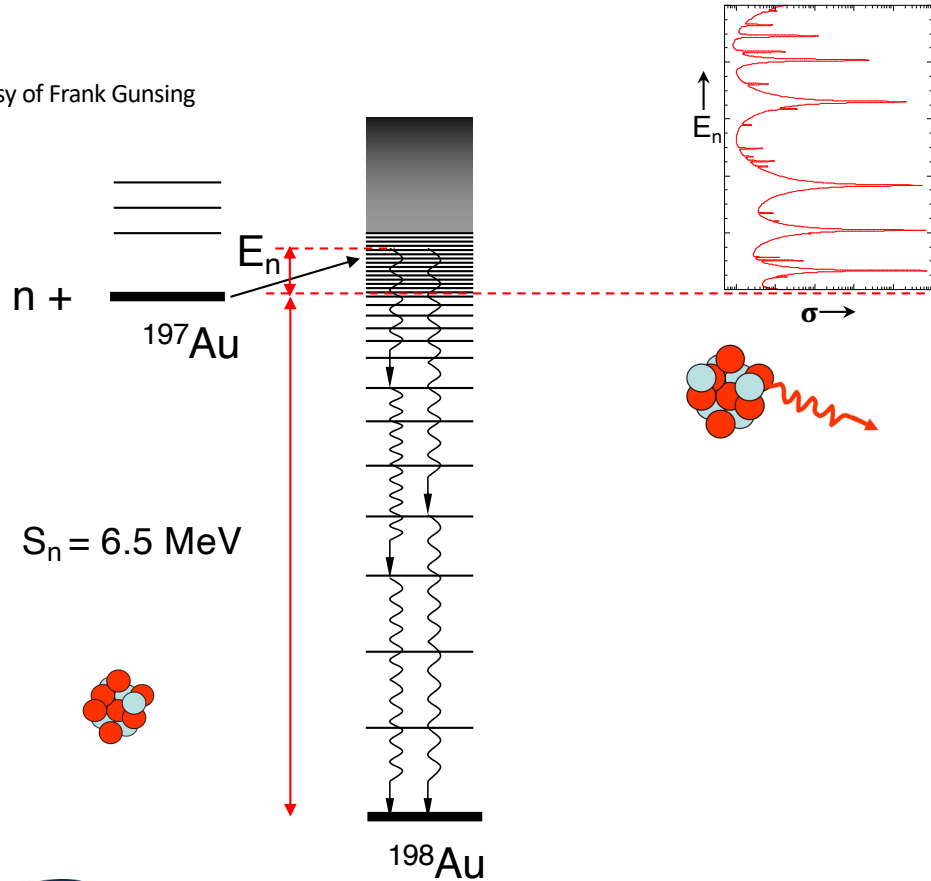
Examples of relevant and/or challenging measurements

❖ $^{197}\text{Au}(n,\gamma)$

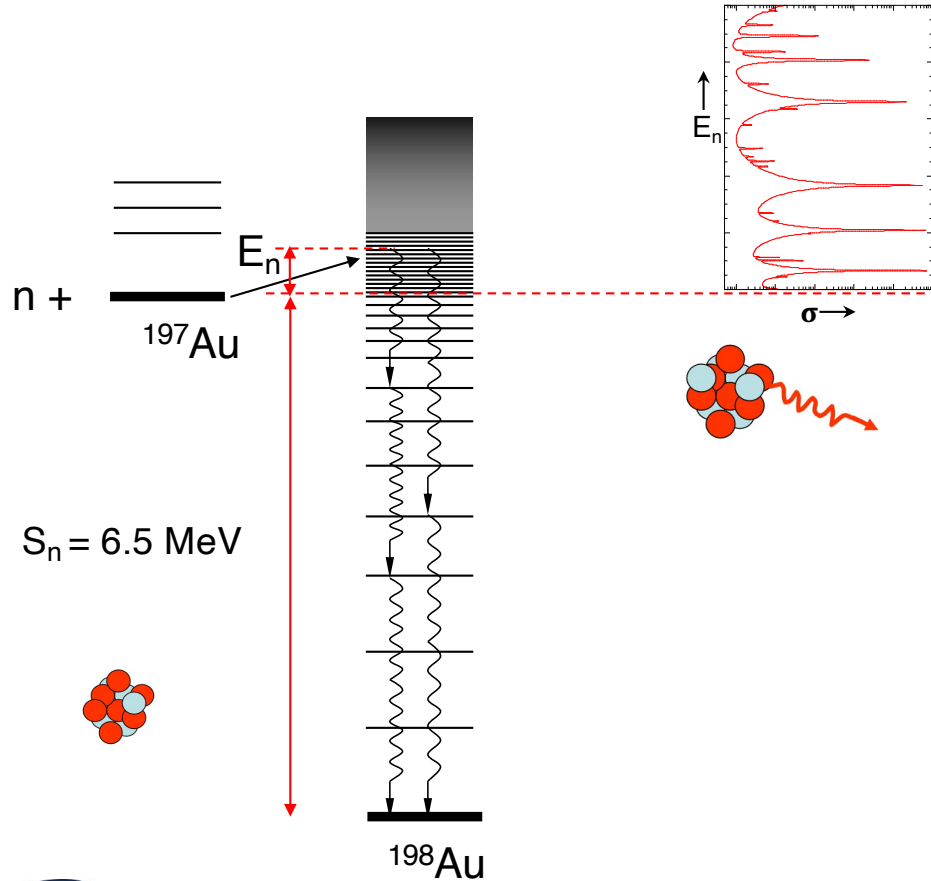
^{195}Tl 1.16 h	^{196}Tl 1.84 h	^{197}Tl 2.84 h	^{198}Tl 5.30 h	^{199}Tl 7.42 h	^{200}Tl 1.09 d	^{201}Tl 3.04 d	^{202}Tl 12.23 d	^{203}Tl 29.524
^{194}Hg 443.96 a	^{195}Hg 10.53 h	^{196}Hg 0.15	^{197}Hg 2.67 d	^{198}Hg 9.97	^{199}Hg 16.87	^{200}Hg 23.1	^{201}Hg 13.18	^{202}Hg 29.86
^{193}Au 17.65 h	^{194}Au 1.58 d	^{195}Au 186.11 d	^{196}Au 6.17 d	^{197}Au 100	^{198}Au 2.70 d	^{199}Au 3.14 d	^{200}Au 48.40 m	^{201}Au 26.00 m
^{192}Pt 0.782	^{193}Pt 50.01 a	^{194}Pt 32.967	^{195}Pt 33.832	^{196}Pt 25.242	^{197}Pt 19.89 h	^{198}Pt 7.163	^{199}Pt 30.80 m	^{200}Pt 12.50 h
^{191}Ir 37.3	^{192}Ir 73.83 d	^{193}Ir 62.7	^{194}Ir 19.28 h	^{195}Ir 2.50 h	^{196}Ir 52.00 s	^{197}Ir 5.80 m	^{198}Ir 8.00 s	^{199}Ir 20.00 s
^{190}Os 26.36	^{191}Os 15.40 d	^{192}Os 40.93	^{193}Os 1.25 d	^{194}Os 6.00 a	^{195}Os 9.00 m	^{196}Os 34.90 m	^{197}Os 2.80 m	

$^{197}\text{Au}(n,\gamma)$, a reference cross section

courtesy of Frank Gunsing

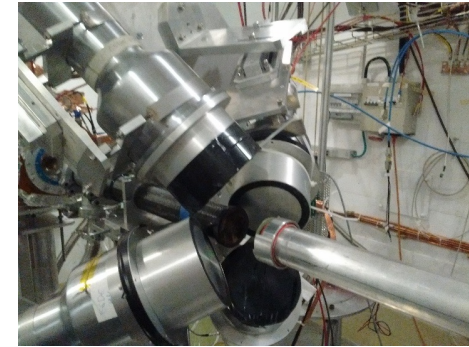


$^{197}\text{Au}(n,\gamma)$, a reference cross section

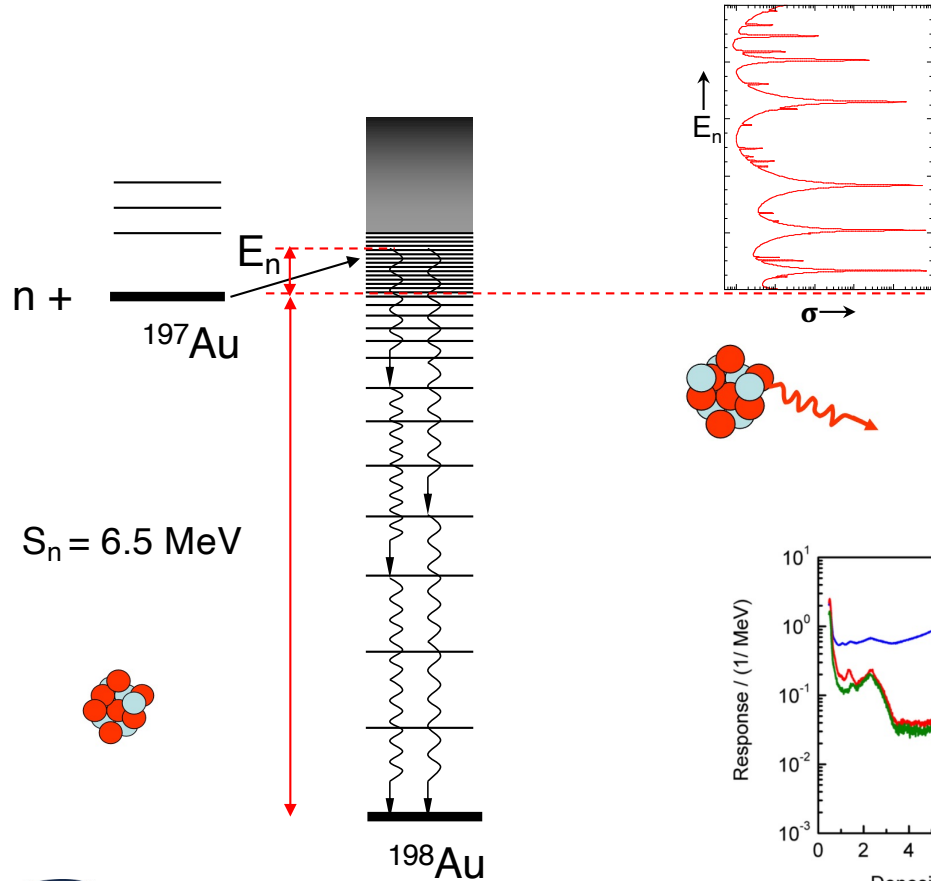


The C_6D_6 Total Energy Detectors (TED)

C_6D_6 scintillators
at 135°

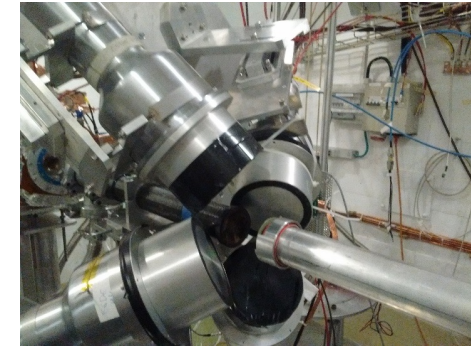


$^{197}\text{Au}(n,\gamma)$, a reference cross section

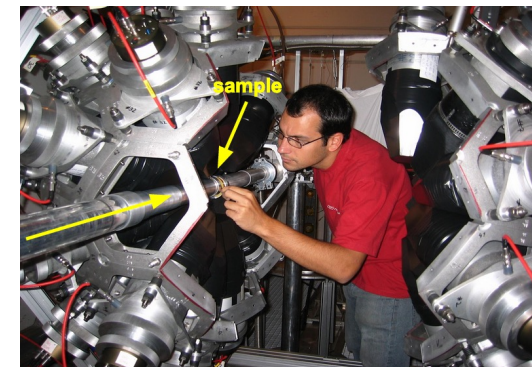
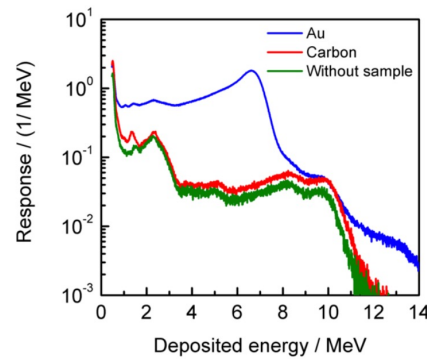


The C_6D_6 Total Energy Detectors (TED)

C_6D_6 scintillators at 135°

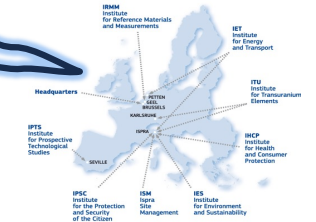


The BaF_2 Total γ -ray Absorption Detector

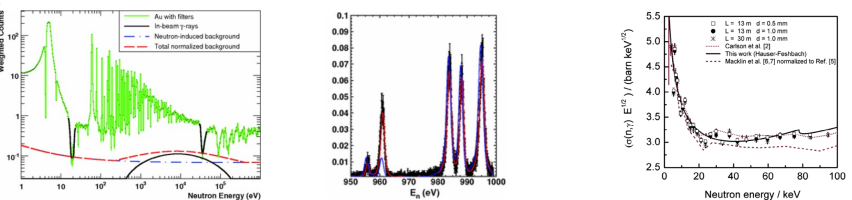


$^{197}\text{Au}(n,\gamma)$, a reference cross section

Cooperation/Collaboration with other facilities: GELINA



C. Massimi, et al., $^{197}\text{Au}(n,\gamma)$ cross section in the resonance region, *Phys. Rev. C* **81** (2010) 044616
 C. Lederer, et al., $\text{Au}197(n,\gamma)$ cross section in the unresolved resonance region, *Phys. Rev. C* **83** (2011) 034608
 C. Massimi, et al., Neutron capture cross section measurements for ^{197}Au from 3.5 to 84 keV at GELINA, *Eur. Phys. J. A* **50** (2014) 124



GELINA @EC-JRC-GEEL

Karlsruhe Astrophysical Database of Nucleosynthesis in Stars

s-process [Standards] [Logbook] [FAQ] [Links] [Contact] p-process

Recommended MACS30 (Maxwellian Averaged Cross Section @ 30keV)

$^{197}\text{Au}(n,\gamma)^{198}\text{Au}$

Total MACS at 30keV: 611.6 ± 6.0 mb

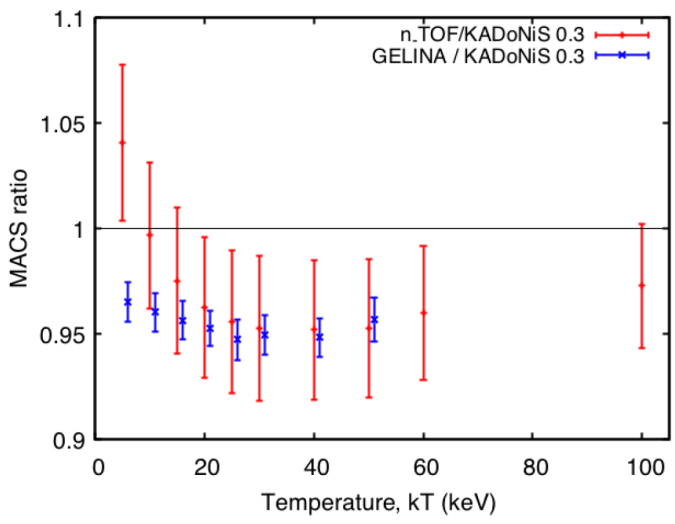
Cross sections do not include stellar enhancement factors!



History

Version	Total MACS [mb]	Partial to gs [mb]	Partial to isomer [mb]
1.0	611.6 ± 6.0	-	-
0.0	582 ± 9	-	-

(Version 0.0 corresponds to Bao et al.)



NPA-X 2022, 4-9 September 2022, CERN

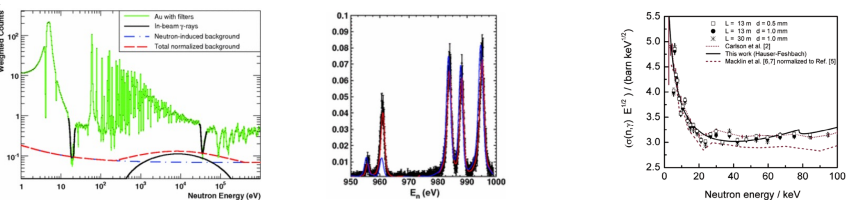
massimi@bo.infn.it

ALMA MATER STUDIORUM UNIVERSITÀ DI BOLOGNA

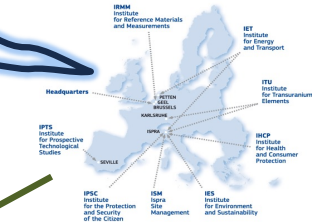
$^{197}\text{Au}(n,\gamma)$, a reference cross section

Cooperation/Collaboration with other facilities: GELINA

- C. Massimi, et al., $^{197}\text{Au}(n,\gamma)$ cross section in the resonance region, [Phys. Rev. C 81 \(2010\) 044616](#)
- C. Lederer, et al., $\text{Au}197(n,\gamma)$ cross section in the unresolved resonance region, [Phys. Rev. C 83 \(2011\) 034608](#)
- C. Massimi, et al., Neutron capture cross section measurements for ^{197}Au from 3.5 to 84 keV at GELINA, [Eur. Phys. J. A 50 \(2014\) 124](#)

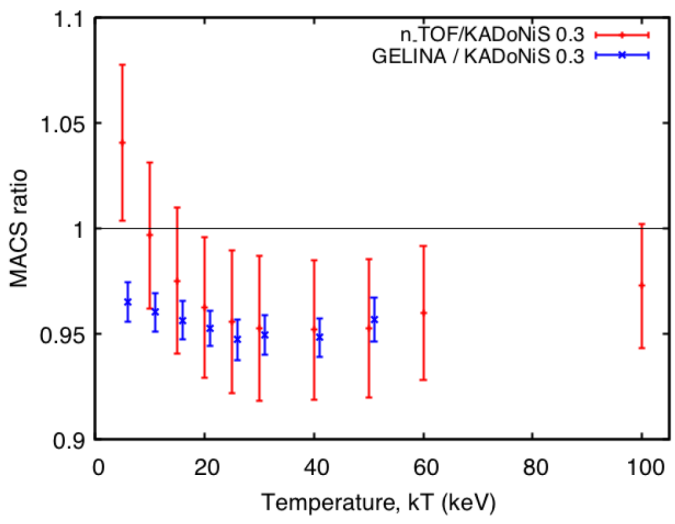


@ NPA – X:
Experimental work at JRC Geel,
by C. Paradelo Dobarro.
Wednesday 7, at 14:45



GELINA @EC-JRC-GEEL

Karlsruhe Astrophysical Database of Nucleosynthesis in Stars



s-process
[Standards] [Logbook] [FAQ] [Links] [Contact]
p-process

▼ Recommended MACS30 (Maxwellian Averaged Cross Section @ 30keV)

$^{197}\text{Au}(n,\gamma)^{198}\text{Au}$

Total MACS at 30keV: 611.6 ± 6.0 mb

▼ History

Version	Total MACS [mb]	Partial to gs [mb]
1.0	611.6 ± 6.0	-
0.0	582 ± 9	-

(Version 0.0 corresponds to Bao et al.)

Most of activation measurements performed so far needs to be renormalized !

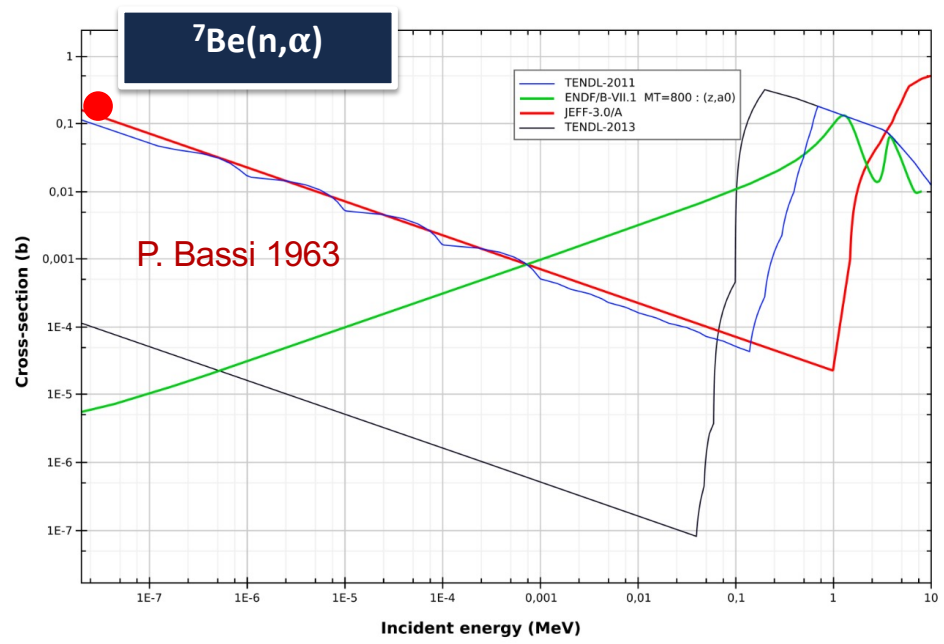
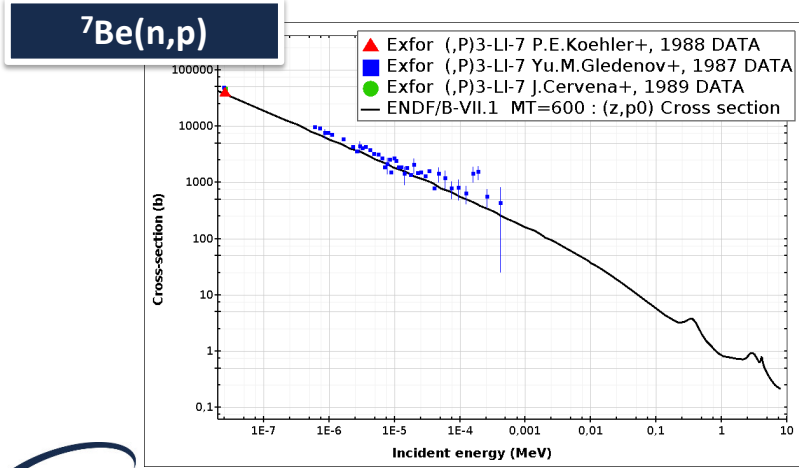
Examples of relevant and/or challenging measurements

❖ ${}^7\text{Be}(n,p)$ & ${}^7\text{Be}(n,\alpha)$



Cosmological lithium problem and ^7Be

- ^7Be is **destroyed** by:
 - $(n,p) \approx 97\%$
 - $(n,\alpha) \approx 2.5\%$
- With a **10 times higher destruction rate** of ^7Be the cosmological lithium problem could be solved (**nuclear solution**)



Data in the literature: scarce and uncertain



NPA-X 2022, 4-9 September 2022, CERN



massimi@bo.infn.it



ALMA MATER STUDIORUM UNIVERSITÀ DI BOLOGNA

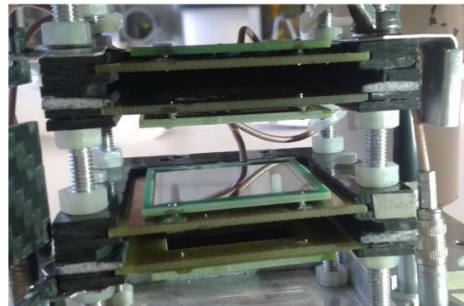
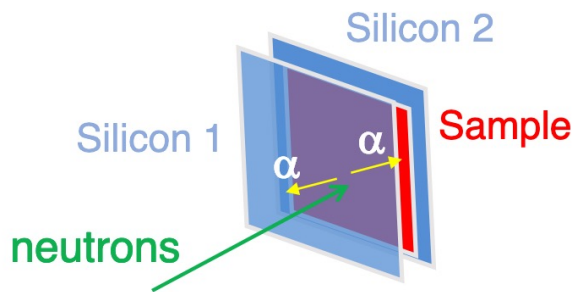
Cosmological lithium problem and ^7Be

The (n,α) reaction produces **two α -particles** emitted back-to-back with **several MeV energy** (Q -value=19 MeV)

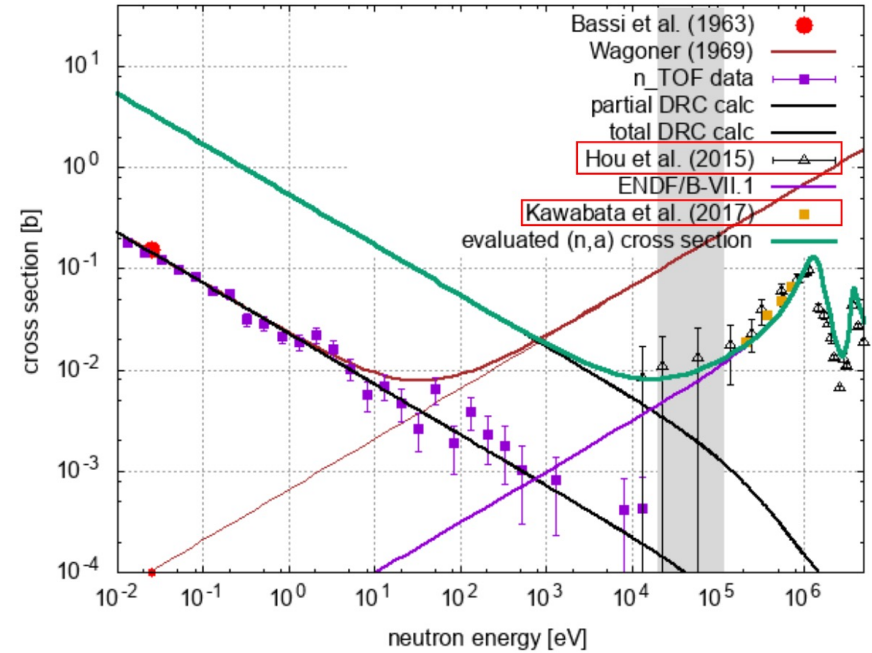
2 Sandwiches of **silicon detector** ($140\ \mu\text{m}, 3\times 3\text{cm}^2$) with ^7Be sample in between **directly inserted in the neutron beam**

Coincidence technique: strong background rejection

$^7\text{Be}(n,\alpha)$



M. Barbagallo *et al.* (The n_TOF Collaboration), [Phys. Rev. Lett. 117 152701 \(2016\)](#)

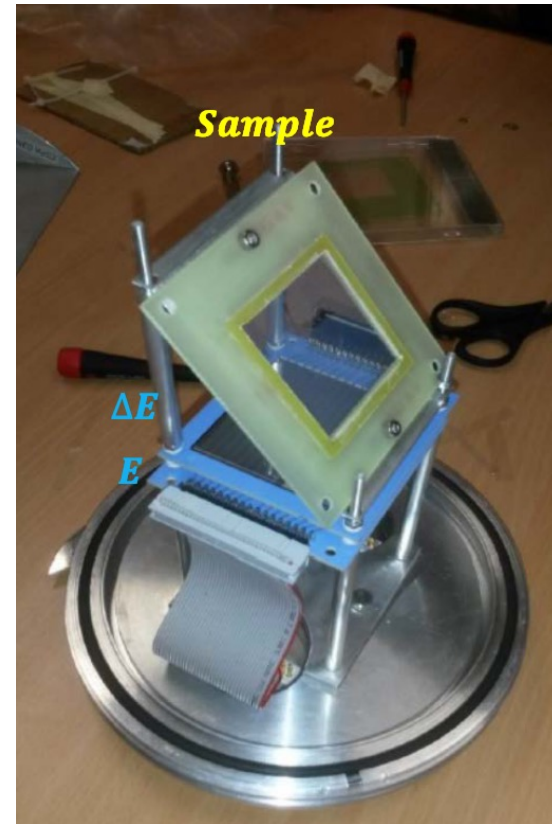
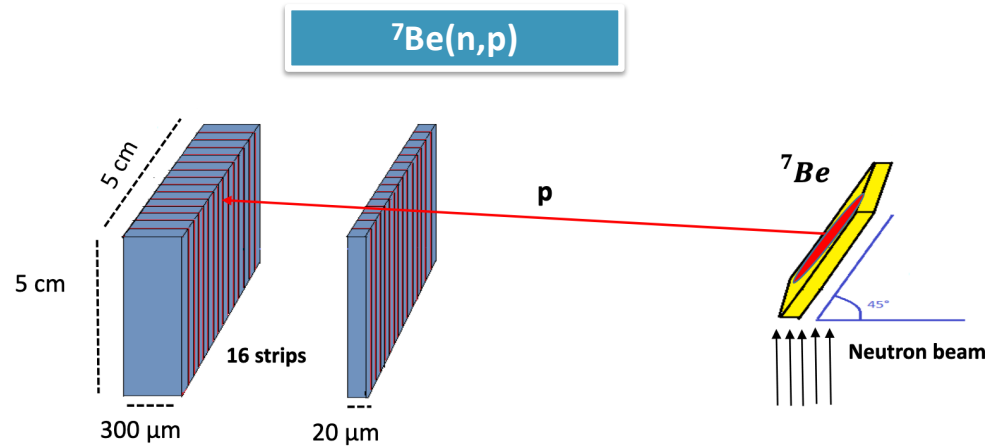


- 4 Electrodeposition on a 5- μm -thick Al foil
- 3 Electrodeposition on a 5- μm -thick Al foil
- 2 droplet deposition on a 0.6- μm -thick polyethylene foil
- 1 droplet deposition on a 0.6- μm -thick polyethylene foil

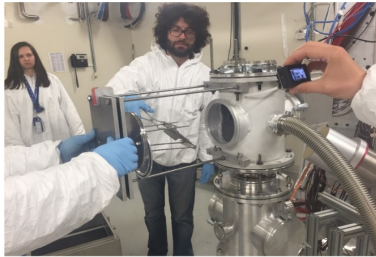


Cosmological lithium problem and ^7Be

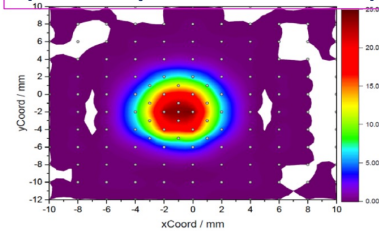
The (n,p) reaction cross section is very high
Q-value=1.6 MeV
Silicon counter telescope ΔE -E
A few ng of 100% **enriched** sample is needed.



Cosmological lithium problem and ^7Be



Sample characterization @PSI
(Gaussian profile 0.5 cm FWHM)

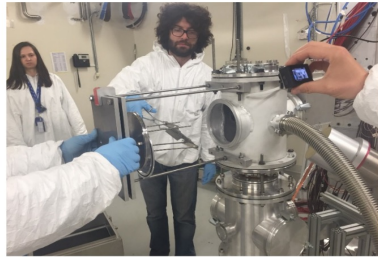


Cooperation/Collaboration
with other facilities:
PSI, ISOLDE

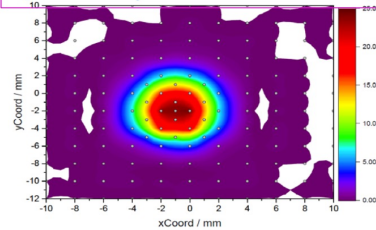
- 200 GBq of ^7Be extracted from the cooling water of the SINQ spallation source at PSI
- Transported to ISOLDE at CERN and installed in the ion source to produce 30 keV ion beam.
- ^7Be beam separated by means of a magnetic dipole, and implanted on a 20 m thick aluminum backing.
- Sample of **1 GBq** ^7Be (~80 ng) transported to EAR2@n_TOF and placed in the neutron beam.

$^7\text{Be}(n,p)$

Cosmological lithium problem and ^7Be

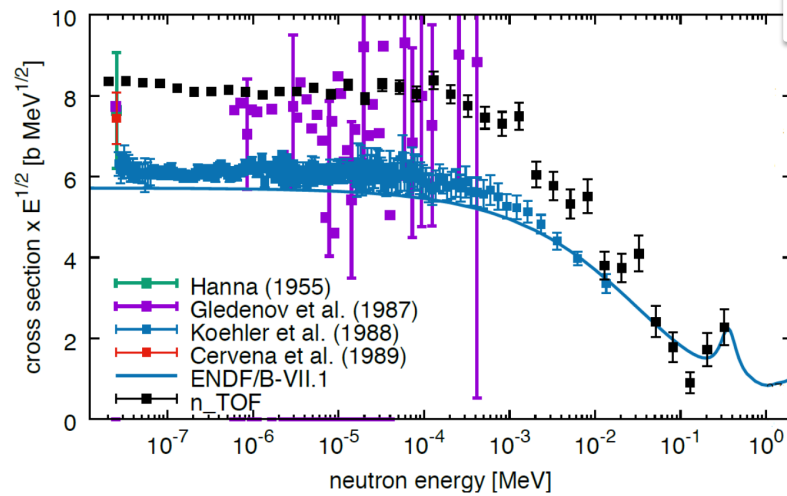


Sample characterization @PSI
(Gaussian profile 0.5 cm FWHM)

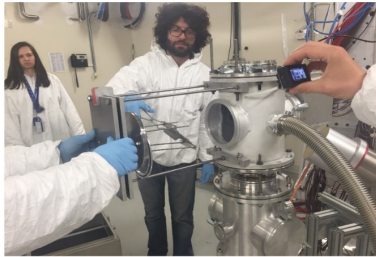


Cooperation/Collaboration
with other facilities:
PSI, ISOLDE

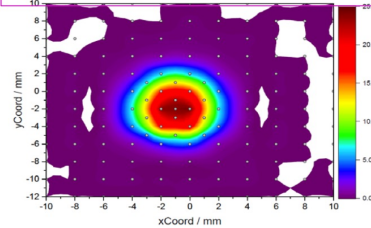
- 200 GBq of ^7Be extracted from the cooling water of the SINQ spallation source at PSI
- Transported to ISOLDE at CERN and installed in the ion source to produce 30 keV ion beam.
- ^7Be beam separated by means of a magnetic dipole, and implanted on a 20 m thick aluminum backing.
- Sample of **1 GBq** ^7Be (~80 ng) transported to EAR2@n_TOF and placed in the neutron beam.



Cosmological lithium problem and ^7Be



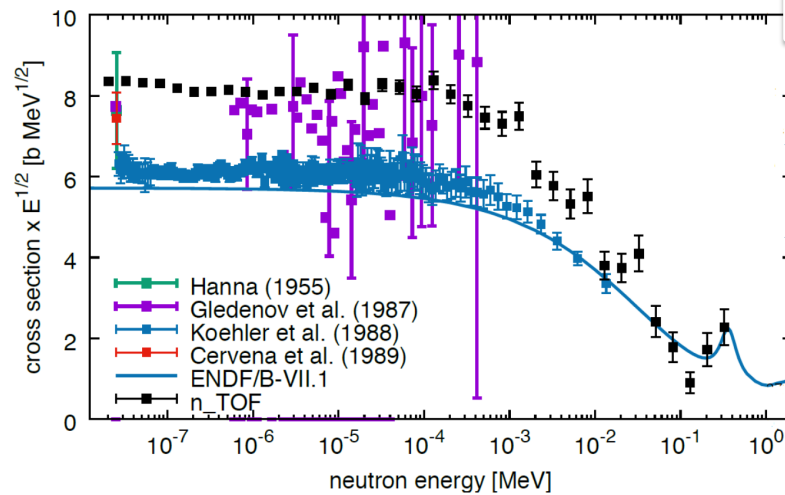
Sample characterization @PSI
(Gaussian profile 0.5 cm FWHM)



Cooperation/Collaboration
with other facilities:
PSI, ISOLDE

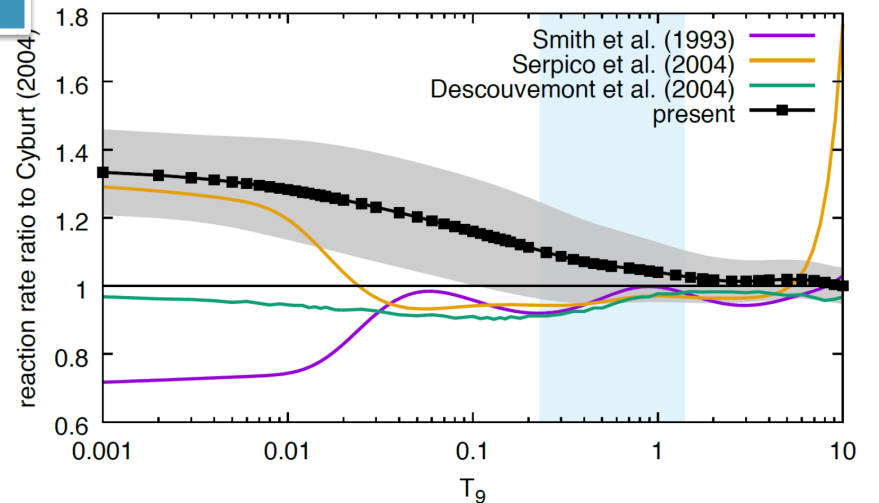
- 200 GBq of ^7Be extracted from the cooling water of the SINQ spallation source at PSI
- Transported to ISOLDE at CERN and installed in the ion source to produce 30 keV ion beam.
- ^7Be beam separated by means of a magnetic dipole, and implanted on a 20 m thick aluminum backing.
- Sample of **1 GBq** ^7Be (~80 ng) transported to EAR2@n_TOF and placed in the neutron beam.

$^7\text{Be}(n,\alpha)$ and $^7\text{Be}(n,p)$
results exclude these
channels as a solution for
the problem



$^7\text{Be}(n,p)$

Reaction rate



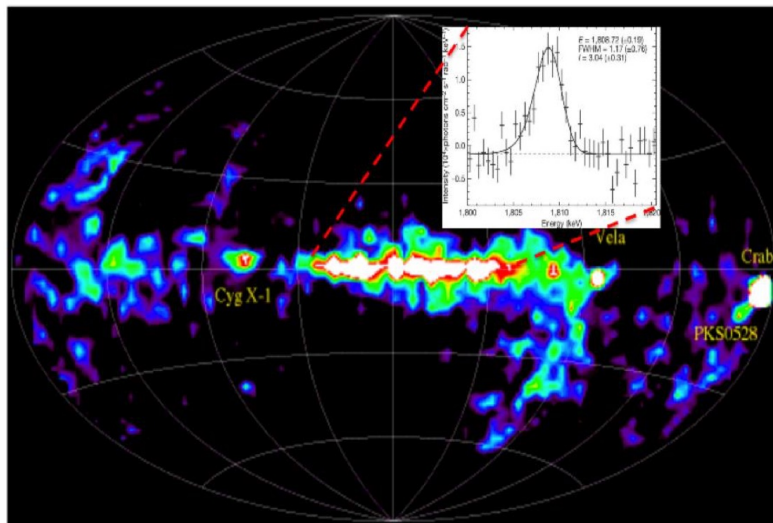
Examples of relevant and/or challenging measurements

❖ $^{26}\text{Al}(n,p)$ & $^{26}\text{Al}(n,\alpha)$



The cosmic γ -ray emitter ^{26}Al

INTEGRAL Measured abundance 2.8(8) Solar Masses
 [R. Diehl, *Nature* **439**, 45(2006)]



C Illiadis et al., *Ast. J. Supp.* **193**, 16 (2011) Sensitivity study of ^{26}Al abundance in Massive stars

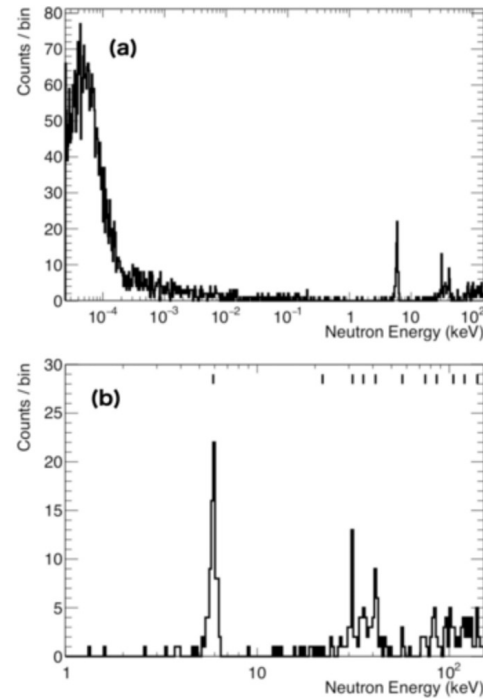
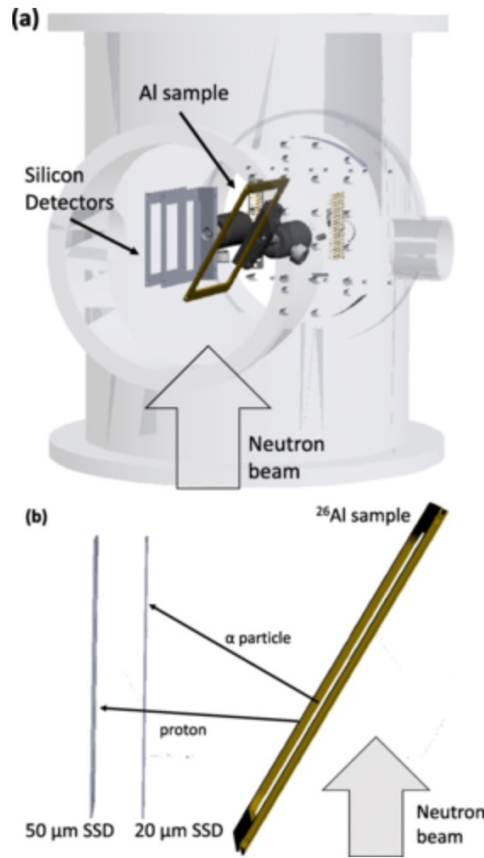
FACTOR CHANGES OF FINAL $^{26}\text{Al}^g$ ABUNDANCE RESULTING FROM REACTION RATE VARIATIONS FOR CONVECTIVE SHELL C/NE BURNING^a, ASSUMING FIVE SPECIES OF ^{26}Al

Reaction ^b	Rate multiplied by						Source ^c	Uncertainty ^d
	100	10	2	0.5	0.1	0.01		
$^{26}\text{Al}^g(n,p)^{26}\text{Mg}$	0.017	0.16	0.63	1.3	1.9	2.0	present	
$^{25}\text{Mg}(p,\gamma)^{26}\text{Al}^g$	2.9	5.4	1.5	0.63	0.35	0.29	il10	5%
$^{25}\text{Mg}(p,\gamma)^{26}\text{Al}^m$	6.7	3.0	0.75	0.71	il10	6%
$^{26}\text{Al}^g(n,\alpha)^{23}\text{Na}$	0.12	0.54	present	
$^{26}\text{Al}^m(n,p)^{26}\text{Mg}$	0.58	present	

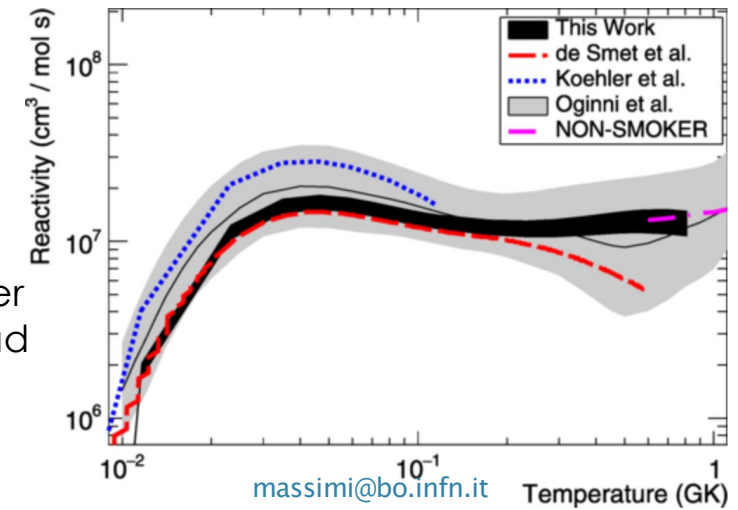
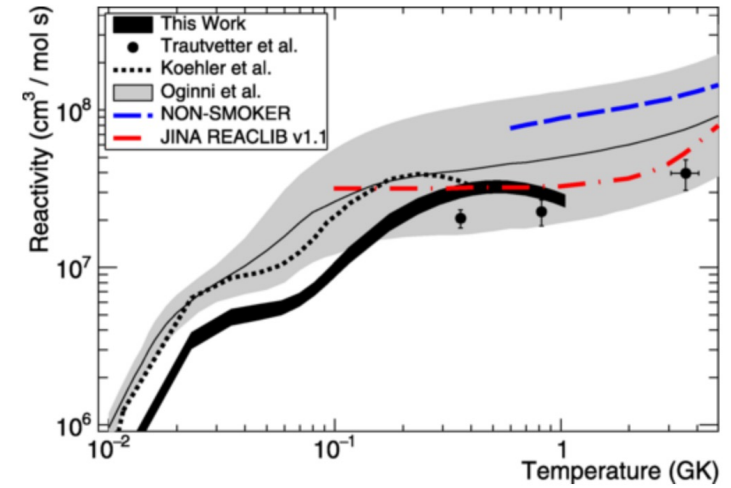
→ $^{26}\text{Al}(n,p)$ and $^{26}\text{Al}(n,\alpha)$ reaction rates represent critical uncertainties for ^{26}Al material processed by explosive and convective burning in massive stars and ejected into the ISM by core collapse supernovae

C. Lederer-Woods *et al.* (The n_TOF Collaboration), [Phys. Rev. C **104** L032803 \(2021\)](#)
 C. Lederer-Woods *et al.* (The n_TOF Collaboration), [Phys. Rev. C **104** L022803 \(2021\)](#)

The cosmic γ -ray emitter ^{26}Al



The astrophysical reactivities are lower than literature data, which would lead to a higher destruction of ^{26}Al



C
o
n
c
l
u
s
i
o
n
s

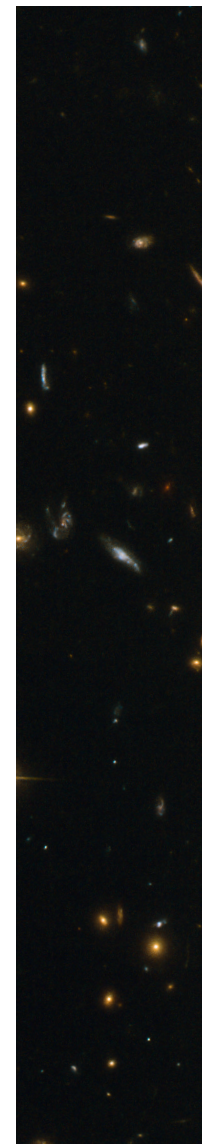
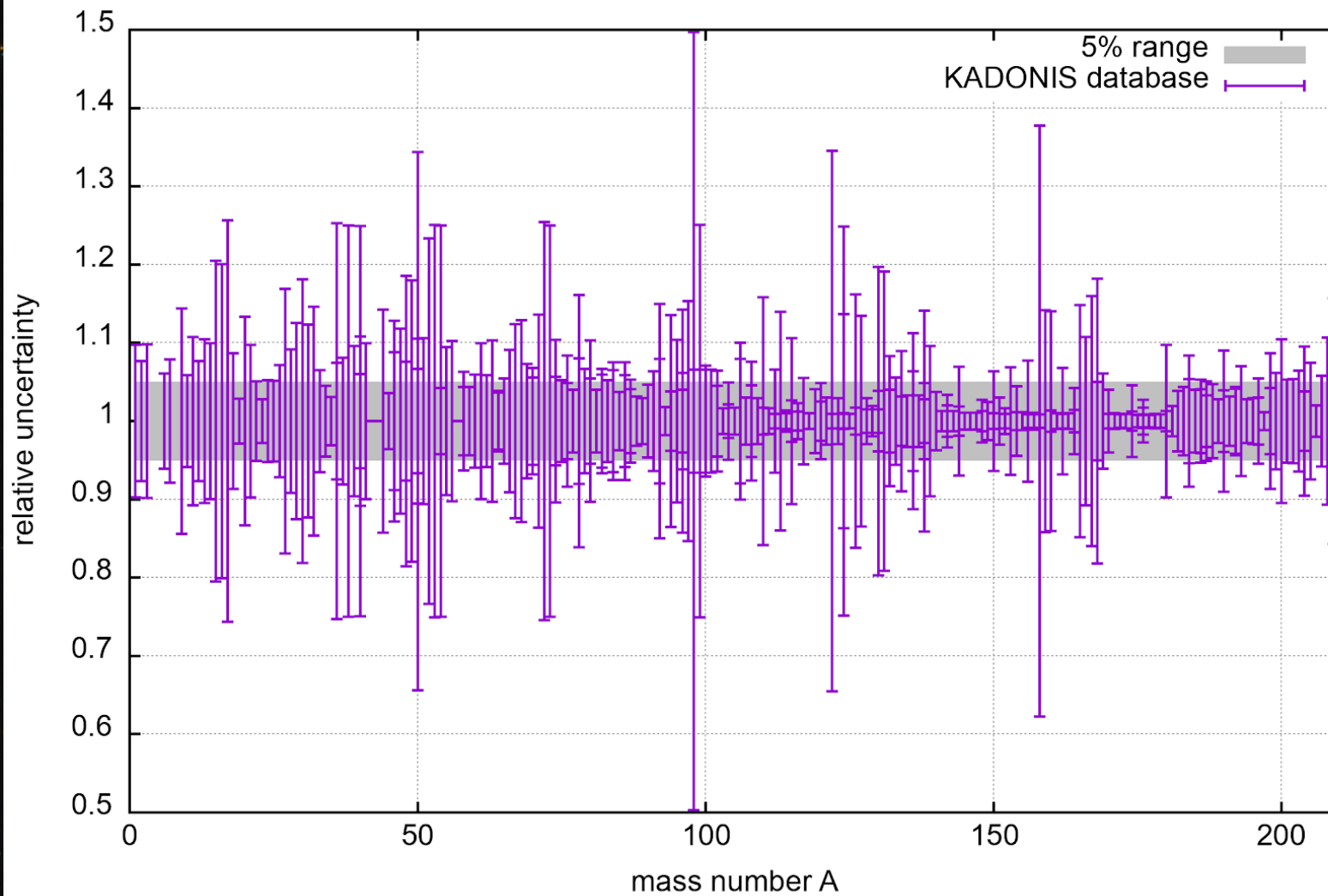


Nuclear Physics in Astrophysics - X

4-9 Sept 2022
CERN

Credit: ESO & ESA/Hubble & NASA

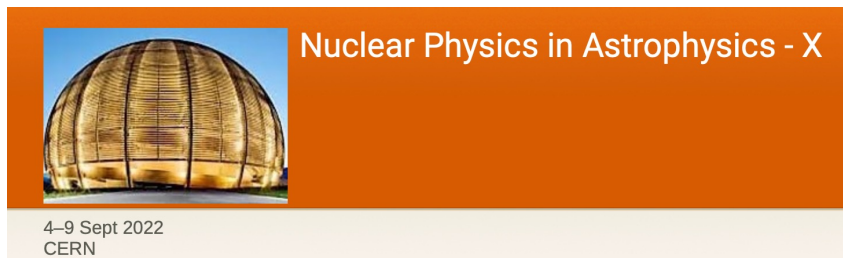
MACS uncertainties



Acknowledgments

Thank you for your attention

Thanks to the organizers



Many thanks to the
n_TOF Collaboration





ALMA MATER STUDIORUM
UNIVERSITÀ DI BOLOGNA

Cristian Massimi

Dipartimento di Fisica e Astronomia

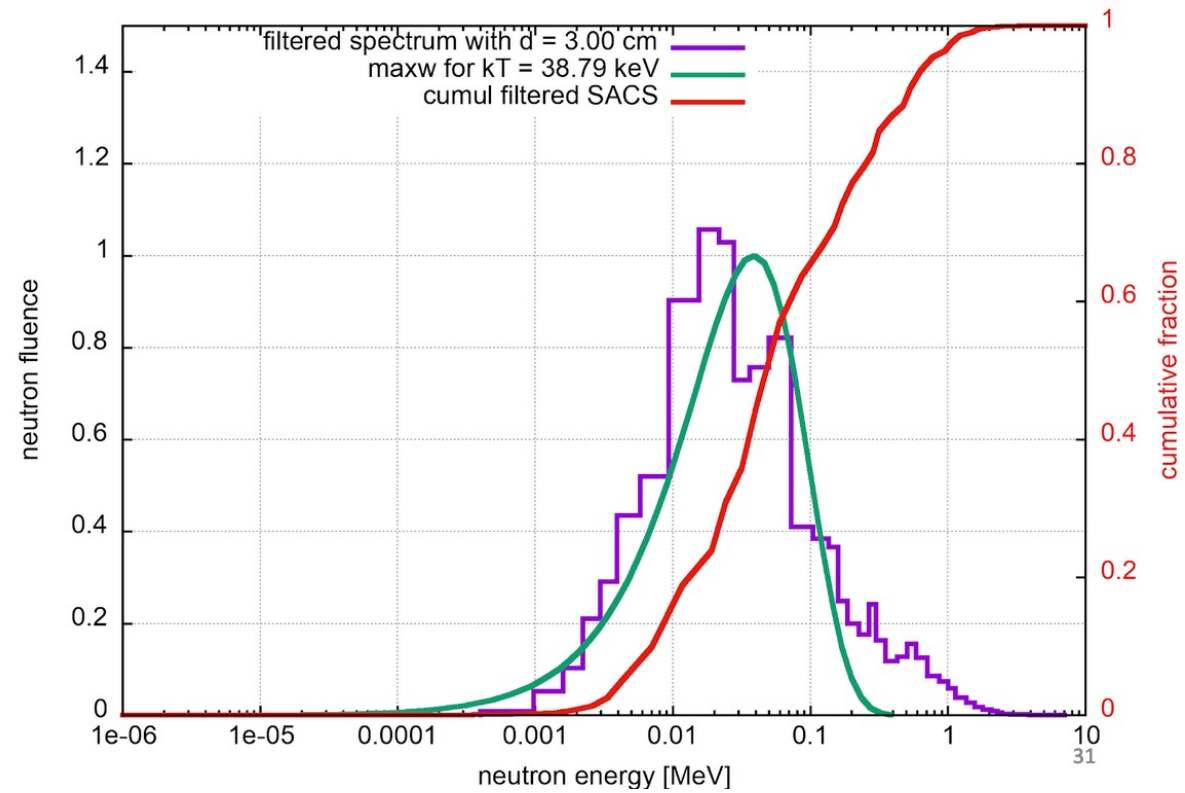
cristian.massimi@unibo.it

www.unibo.it

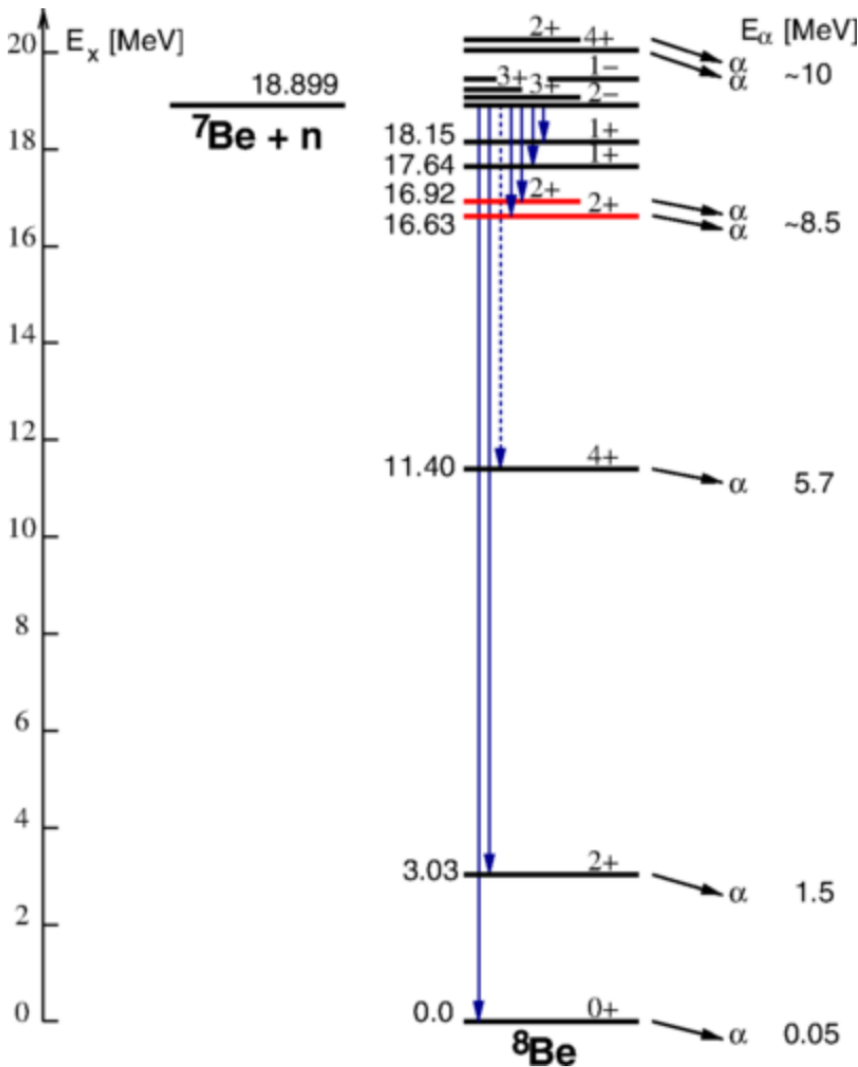
Backup (NEAR)

The NEAR Station

SACS for Au197 (ENDF/B-VIII.0 data)



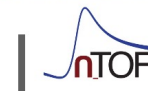
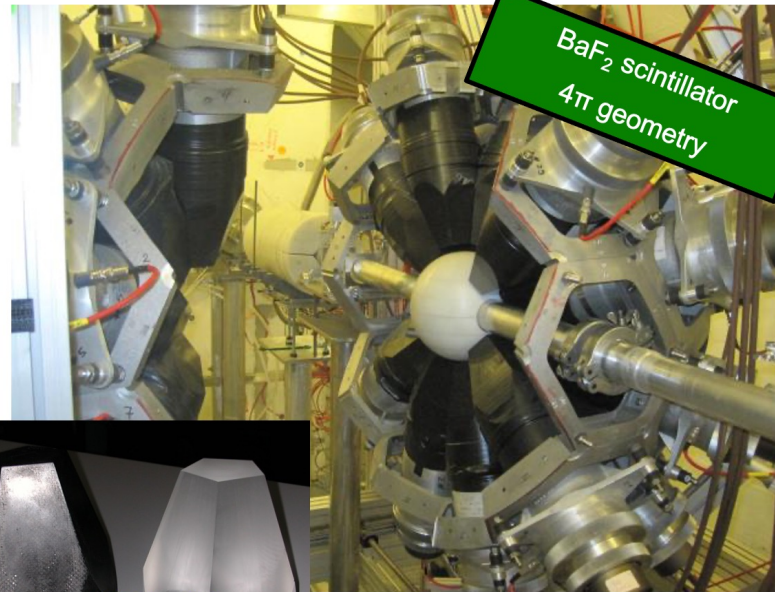
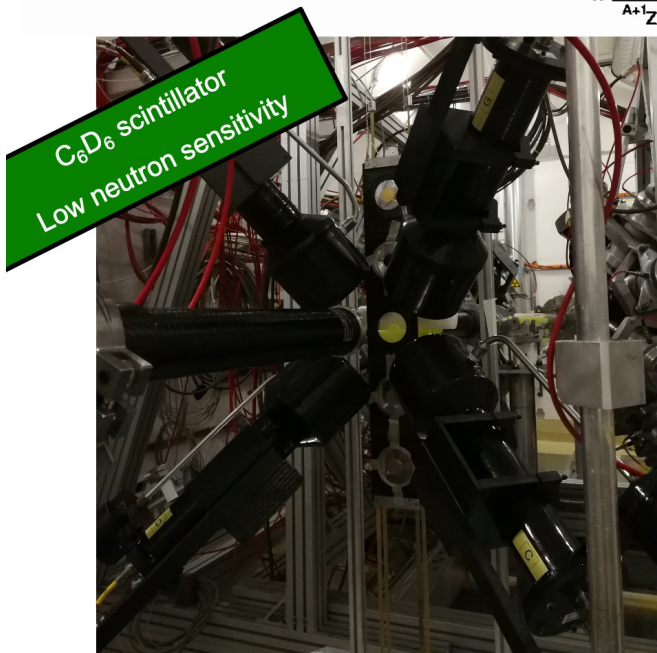
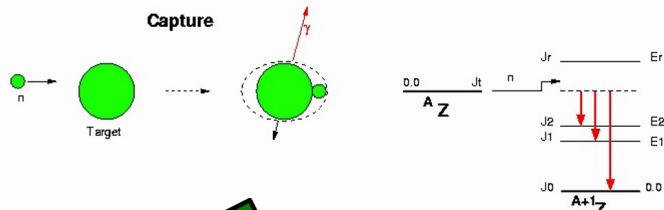
Backup (⁷Be)



Backup

Detectors for (n,γ) reaction

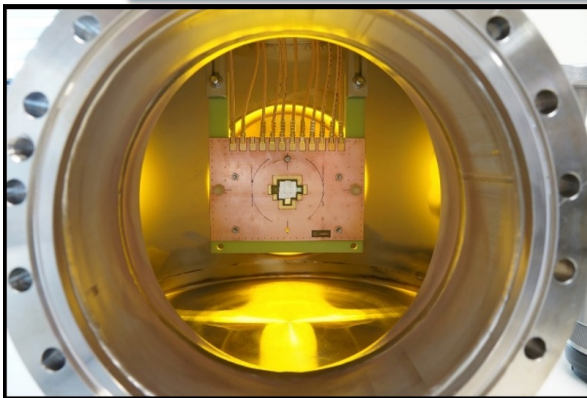
Capture reactions are measured by detecting γ -rays emitted in the de-excitation process. **Two different systems**, to minimize different types of background



Backup

Detectors: (n,p) and (n, α) reactions

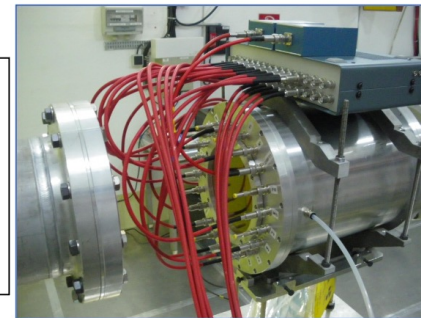
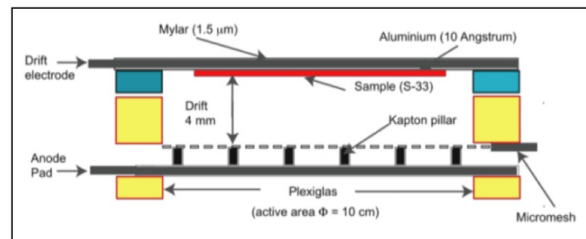
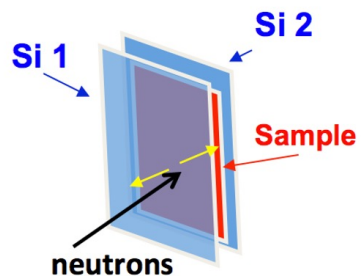
Gas and solid state detectors are used for detecting charged particles, depending on the energy region of interest and the Q-value of the reaction



Silicon detectors
Silicon sandwich
Diamond detector
 ΔE -E Telescopes

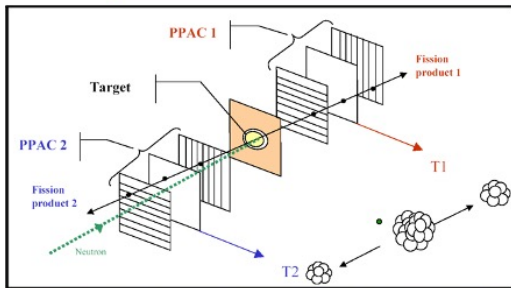
Micromegas chamber

- low-noise, high-gain, radiation-hard detector



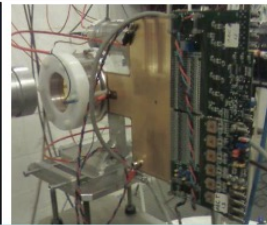
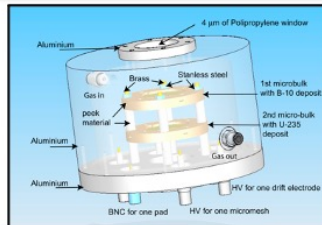
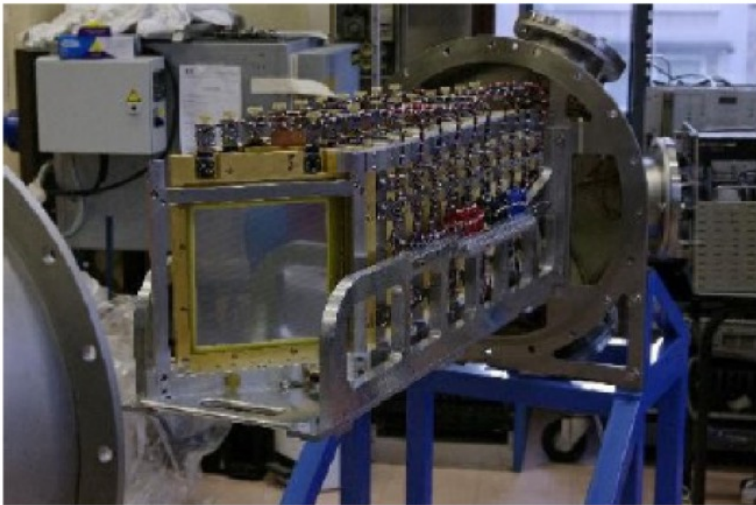
Backup

Several systems have been used for detecting fission fragments.
The main **problem** in fission measurements is the **background** due to α -decay.



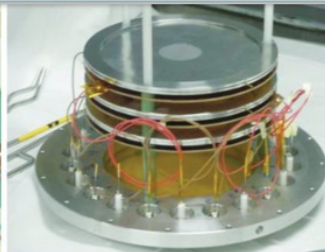
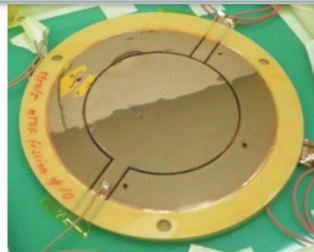
Parallel Plate Avalanche Counters (PPAC)

- Fission fragments detected **in coincidence**
- Very good rejection of α -background



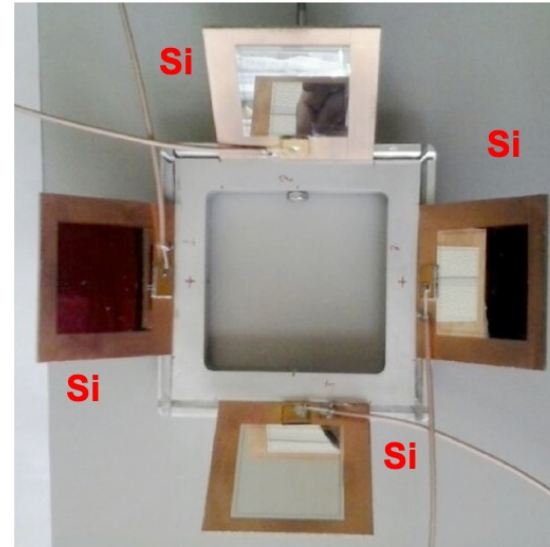
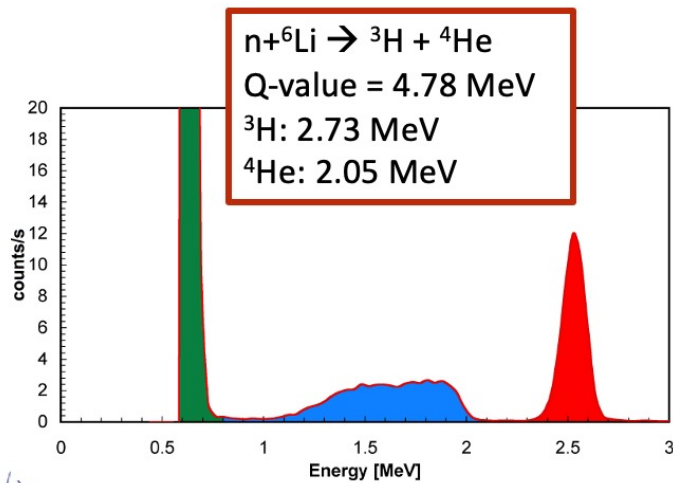
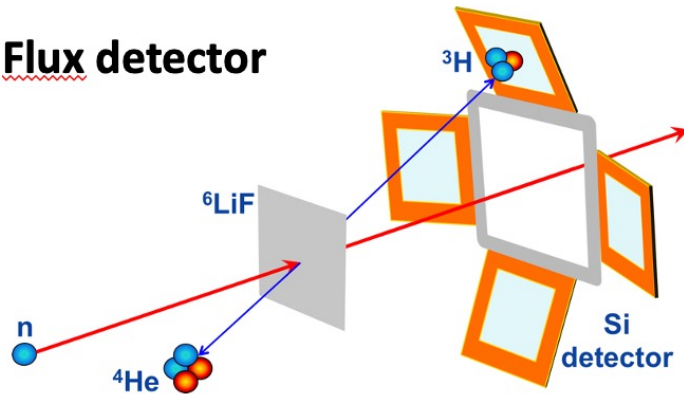
Micromegas chamber

- **low-noise, high-gain, radiation-hard detector**

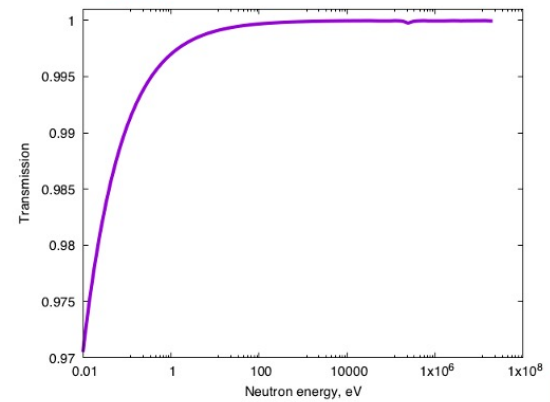


Backup

Flux detector

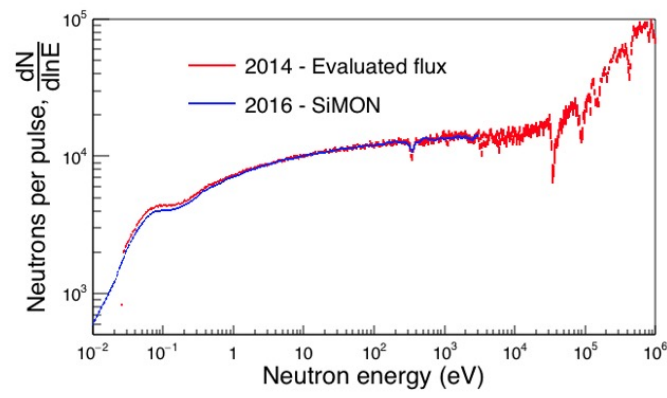
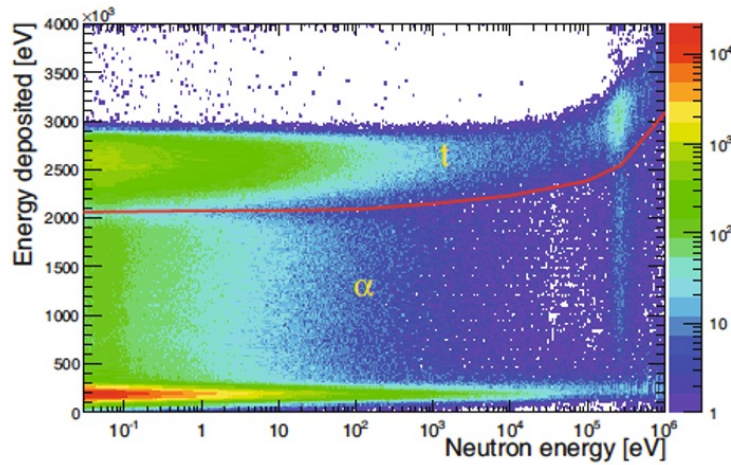
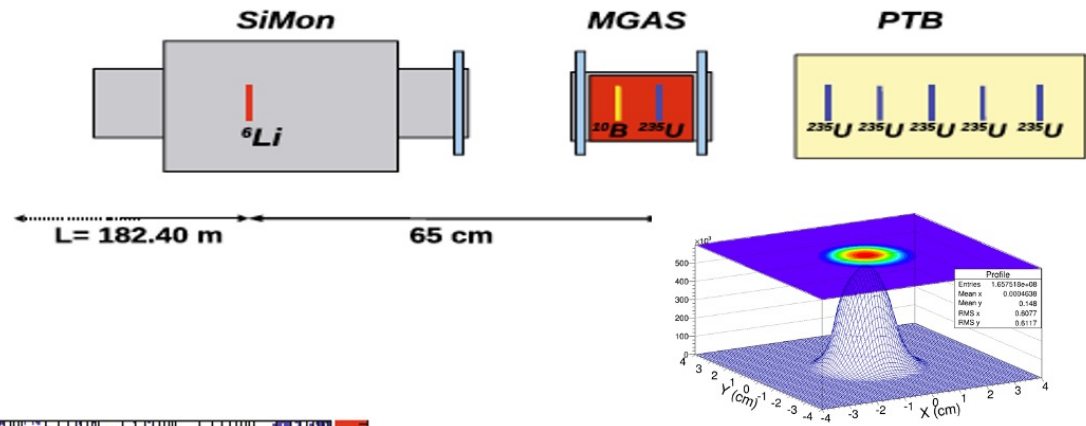


MSX09-3007 3 cm × 3 cm,
300 μm thick > particle range

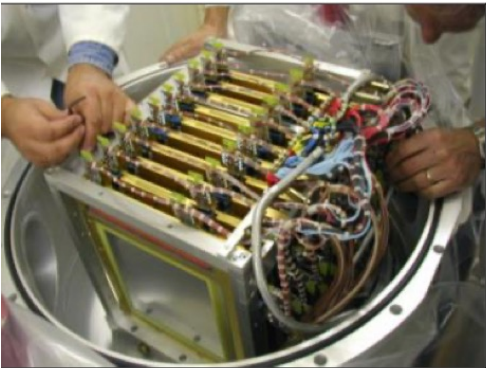


Backup

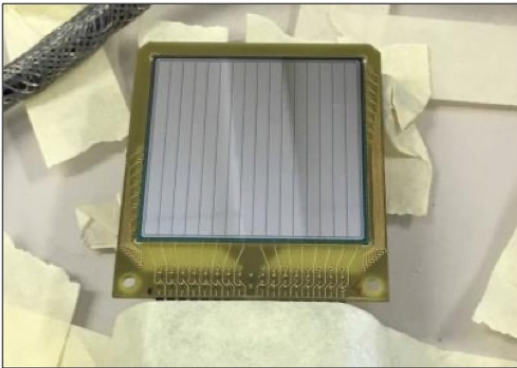
3 different detectors based on 3 neutron standards



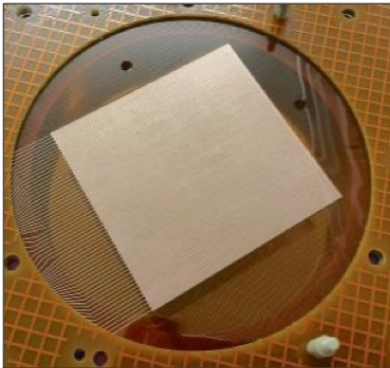
Backup



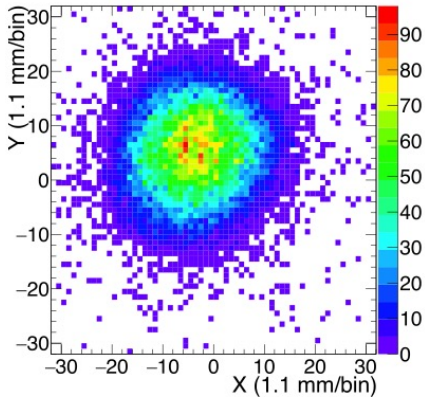
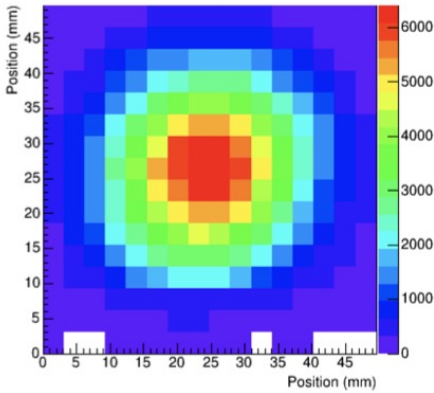
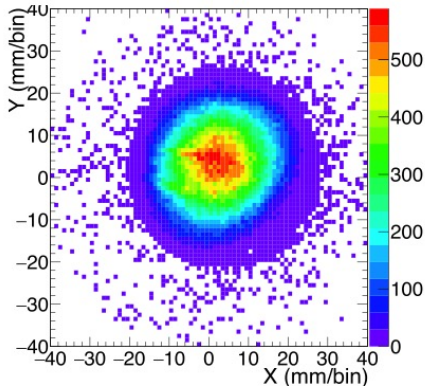
PPAC



SiMon2D



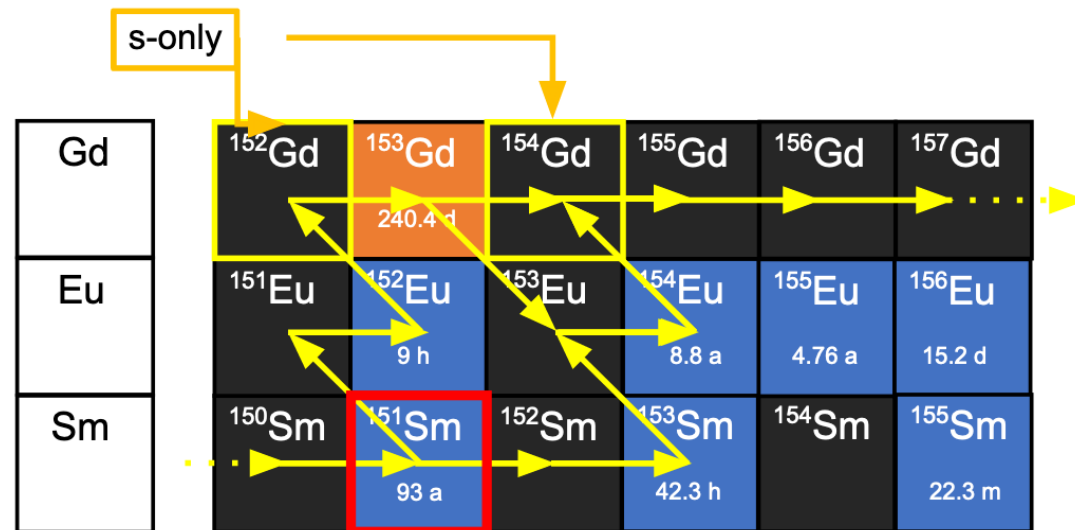
XY MicroMegas





s-process branching at ^{151}Sm

- ❖ branching isotope in the Sm-Eu-Gd region: test for low-mass TP-AGB H-burning 10^8 K, He-Shell flashes $2.5\text{-}2.8 \times 10^8$ K
- ❖ branching ratio (capture/ β -decay) provides information on the thermodynamical conditions of the s-processing (if accurate capture rates are known!)



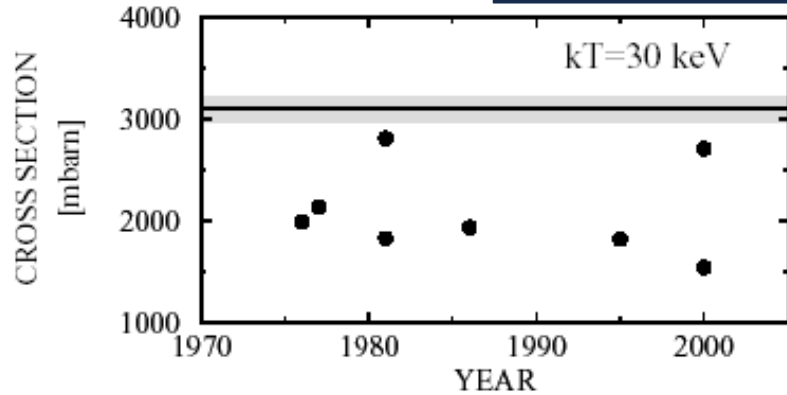
small samples

180 mg of ^{151}Sm

184 GBq

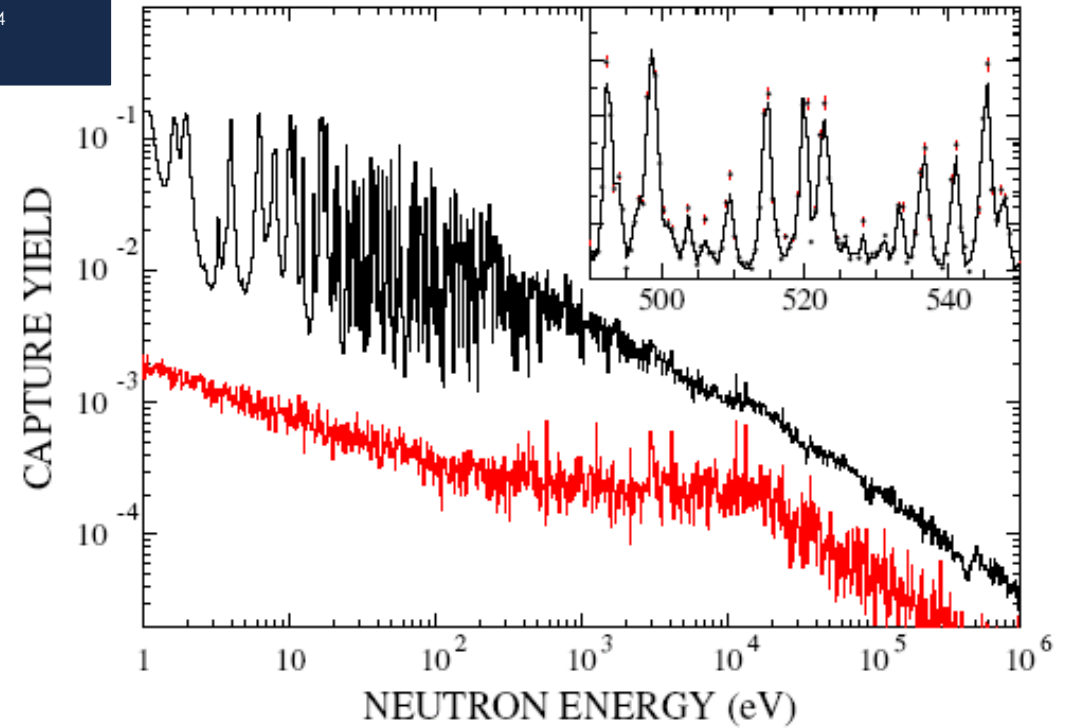
$^{151}\text{Sm}(n,\gamma)$

MACS-30 = 3100 ± 160 mb
 $\langle D_0 \rangle = 1.48 \pm 0.04$ eV,
 $S_0 = (3.87 \pm 0.20) \times 10^{-4}$
 $\langle \Gamma_\gamma \rangle = 108 \pm 15$ meV



Gd 151 120 d ϵ : α 2.60 γ 154; 243; 175...	Gd 152 0.20 $1.1 \cdot 10^{14}$ a	Gd 153 239.47 d ϵ : γ 97; 103; 70... α 20000 $\sigma_{n,\alpha}$ 0.03	Gd 154 2.18 σ 60	Gd 155 14.80 σ 61000 $\sigma_{n,\alpha}$ 0.00008	Gd 156 20.47 $\sigma \sim 2.0$	Gd 157 15.65 σ 254000 $\sigma_{n,\alpha} < 0.05$
Eu 150 12.8 h / 36.9 a β^- 1.0 ϵ : γ 334; 439; 407	Eu 151 47.81 σ 4 + 3150 + 6000	Eu 152 96 m / 9.3 h / 13.33 a β^- 1.3; ϵ 3 β^- 0.8; 1.8 ϵ : γ 841; 963; 944; 9800; 11000	Eu 153 52.19 σ 300 $\sigma_{n,\alpha}$ 1E-6	Eu 154 46.0 m / 8.8 a β^- 0.8; 1.8 ϵ : γ 123; 1274; 723; 1005; 101...	Eu 155 4.761 a β^- 0.17; 0.25... γ 87; 105... σ 3900	Eu 156 15.2 d β^- 0.5; 2.4... γ 812; 89; 1231...
Sm 149 13.82 σ 40100 $\sigma_{n,\alpha}$ 0.031	Sm 150 7.38 σ 102	Sm 151 93 a β^- 0.1... γ (22...); e^- σ 15200	Sm 152 26.75 σ 206	Sm 153 46.27 h β^- 0.7; 0.8... γ 103; 70... σ 420	Sm 154 22.75 σ 7.5	Sm 155 22.4 m β^- 1.5... γ 104; 246; 141...

U Abbondanno *et al.* (The n_TOF Collaboration), [Phys. Rev. Lett. 93, 161103 \(2004\)](#)
 S. Marrone *et al.*, (The n_TOF Collaboration) [Phys. Rev. C 73, 034604 \(2006\)](#)

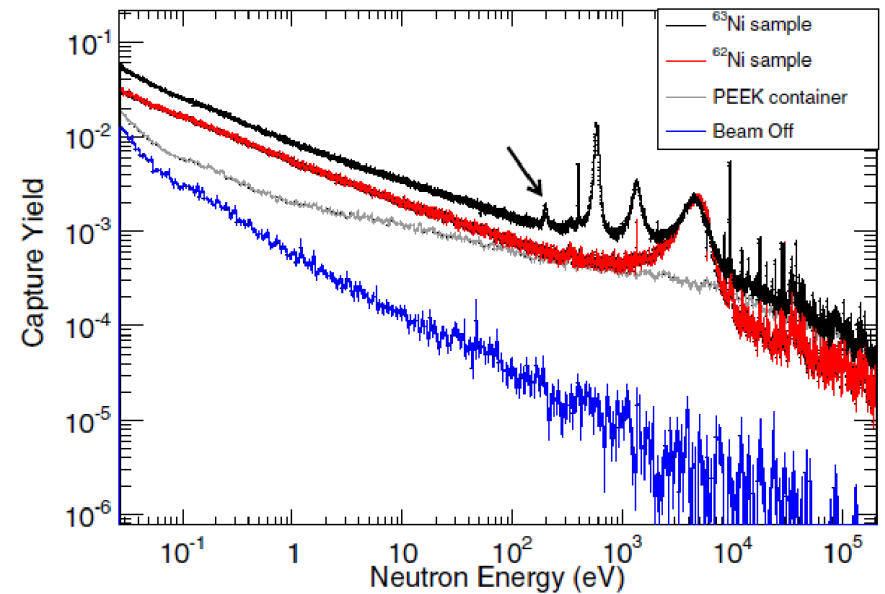


- enhancement of the ^{154}Gd yields in AGB's: 91% wrts, while ^{152}Gd is at 78% wrts
- remaining uncertainty is the β -decay rate of ^{151}Sm

s-process branching at ^{63}Ni

Zn 60 2.4 m β^+ 2.5; 3.1... γ 670; 61; 273; 334...	Zn 61 1.5 m β^+ 4.4... γ 475; 1660; 970...	Zn 62 9.13 h ϵ β^+ 0.7 γ 41; 597; 548; 508...	Zn 63 38.1 m β^+ 2.3... γ 670; 962; 1412...	Zn 64 48.268 σ 0.74 $\sigma_{n,\alpha}$ $1.1E-5$ $\sigma_{n,p}$ $<1.2E-5$	Zn 65 244.3 d ϵ ; β^- 0.3 γ 1115... σ 66 $\sigma_{n,\alpha}$ 2.0	Zn 66 27.975 σ 0.9 $\sigma_{n,\alpha}$ $<2E-5$	Zn 67 4.102 σ 6.9 $\sigma_{n,\alpha}$ 0.0004
Cu 59 82 s β^+ 3.8... γ 1302; 878; 339; 465...	Cu 60 23 m β^+ 2.0; 3.9... γ 1332; 1792; 826...	Cu 61 3.4 h β^+ 1.2... γ 283; 656; 67; 1186...	Cu 62 9.74 m β^+ 2.9... γ (1173...)	Cu 63 69.15 σ 4.5	Cu 64 12 700 h ϵ ; β^- 0.5 β^+ 0.7 γ (1346) σ ~270	Cu 65 3.85 σ 2.17	Cu 66 5.1 m β^- 2.6... γ 1039; (834...) σ 140
Ni 58 68.0769 σ 4.6 $\sigma_{n,\alpha}$ <0.00003	Ni 59 $7.5 \cdot 10^4$ a ϵ ; β^+ ... no γ ; σ 77.7 $\sigma_{n,\alpha}$ 14; $\sigma_{n,p}$ 2 σ_{abs} 92	Ni 60 26.2231 σ 2.9	Ni 61 1.1399 σ 2.5 $\sigma_{n,\alpha}$ 0.00003	Ni 62 3.6345 σ 15	Ni 63 100 a β^- 0.07 no γ σ 20	Ni 64 0.9256 σ 1.6	Ni 65 2.52 h γ 1482; 1115; 366... σ 22

C Lederer *et al.* (The n_TOF Collaboration), [Phys. Rev. Lett. 110, 022501 \(2013\)](#)
 C Lederer *et al.* (The n_TOF Collaboration), [Phys. Rev. C 89, 025810 \(2014\)](#)



1156 mg (ILL), 12% ^{63}Ni (240 GBq)

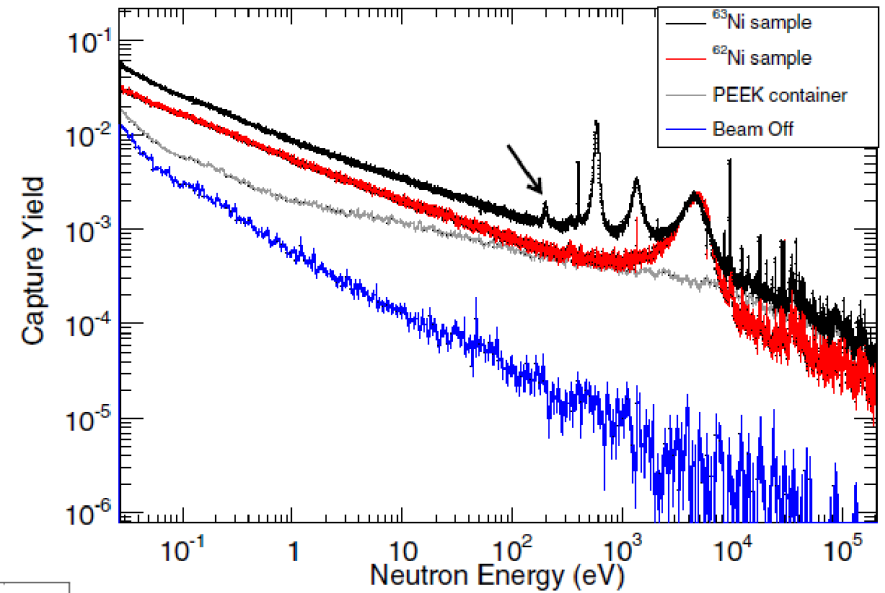
first experimental data on $^{63}\text{Ni}(n,\gamma)$ at astrophysical relevant energies

MACS = 66.7 (18.7) mb, a factor 2 higher wrt previous estimations

s-process branching at ^{63}Ni

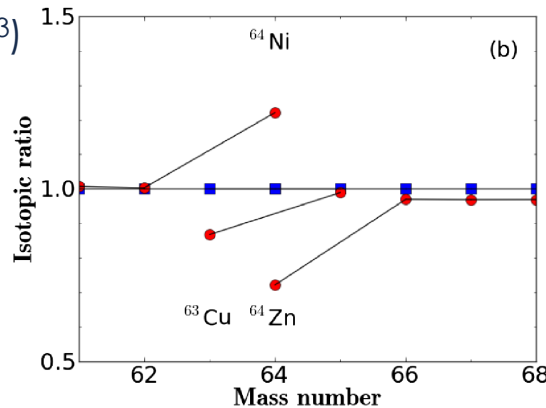
Zn 60 2.4 m β^+ 2.5; 3.1... γ 670; 61; 273; 334...	Zn 61 1.5 m β^+ 4.4... γ 475; 1660; 970...	Zn 62 9.13 h ϵ 0.7 γ 41; 597; 548; 508...	Zn 63 38.1 m β^+ 2.3... γ 670; 962; 1412...	Zn 64 48.268 σ 0.74 $\sigma_{n,\alpha}$ 1.1E-5 $\sigma_{n,p}$ <1.2E-5	Zn 65 244.3 d ϵ ; β^- 0.3 γ 1115... σ 66 $\sigma_{n,\alpha}$ 2.0	Zn 66 27.975 σ 0.9 $\sigma_{n,\alpha}$ <2E-5	Zn 67 4.102 σ 6.9 $\sigma_{n,\alpha}$ 0.0004
Cu 59 82 s β^+ 3.8... γ 1302; 878; 339; 465...	Cu 60 23 m β^+ 2.0; 3.9... γ 1332; 1792; 826...	Cu 61 3.4 h β^+ 1.2... γ 283; 656; 67; 1186...	Cu 62 9.74 m β^+ 2.9... γ (1173...)	Cu 63 69.15 σ 4.5	Cu 64 12 700 h ϵ ; β^- 0.7 γ (1346) σ ~270	Cu 65 3.85 σ 2.17	Cu 66 5.1 m β^- 2.6... γ 1039; (834...) σ 140
Ni 58 68.0769 σ 4.6 $\sigma_{n,\alpha}$ <0.00003	Ni 59 7.5 · 10 ⁴ a ϵ ; β^+ ... no γ ; σ 77.7 $\sigma_{n,\alpha}$ 14; $\sigma_{n,p}$ 2 σ_{abs} 92	Ni 60 26.2231 σ 2.9	Ni 61 1.1399 σ 2.5 $\sigma_{n,\alpha}$ 0.00003	Ni 62 3.6345 σ 15	Ni 63 100 a β^- 0.07 no γ σ 20	Ni 64 0.9256 σ 1.6	Ni 65 2.52 h γ 1482; 1115; 366... σ 22

C Lederer *et al.* (The n_TOF Collaboration), [Phys. Rev. Lett. 110, 022501 \(2013\)](#)
 C Lederer *et al.* (The n_TOF Collaboration), [Phys. Rev. C 89, 025810 \(2014\)](#)



Core He-burning (300 MK, 10⁷cm⁻³)

Shell C-burning (1GK, 10¹¹⁻¹²cm⁻³)



- Constrain the weak s-process inventory in ^{63}Cu , ^{64}Ni and ^{64}Zn before SN explosion takes place

$^{22}\text{Ne}(\alpha, n)^{25}\text{Mg}$

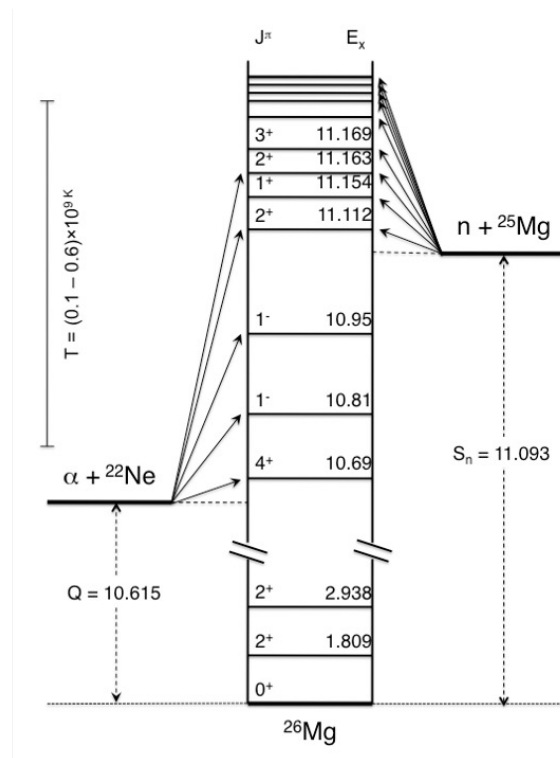
Element	Spin / parity
^{22}Ne	0^+
^4He	0^+

Only **natural-parity states in ^{26}Mg** can participate in the $^{22}\text{Ne}(\alpha, n)^{25}\text{Mg}$ reaction

$$J^\pi = 0^+, 1^-, 2^+, 3^-, 4^+ \dots$$

$$\vec{J} = \underbrace{\vec{I} + \vec{i}}_{\vec{J} = 0} + \vec{\ell} \quad \pi = (-1)^\ell$$

Study of ^{26}Mg levels via $n + ^{25}\text{Mg}$



$n + ^{25}\text{Mg}$

Element	Spin/parity
^{25}Mg	$5/2^+$
neutron	$1/2^+$

s-wave $\rightarrow J^\pi = 2^+, 3^+$

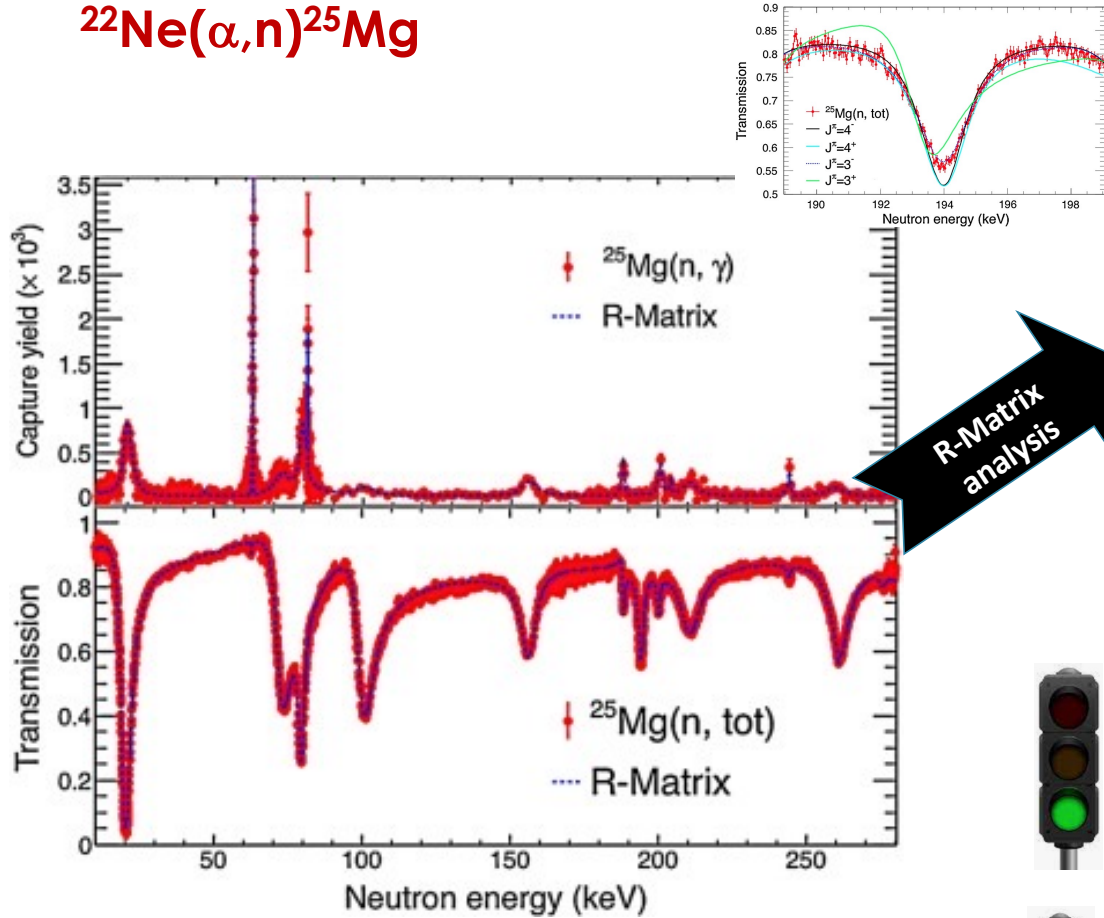
p-wave $\rightarrow J^\pi = 1^-, 2^-, 3^-, 4^-$

d-wave $\rightarrow J^\pi = 0^+, 1^+, 2^+, 3^+, 4^+, 5^+$

$$\vec{J} = \underbrace{\vec{I} + \vec{i}}_{\vec{J} = 2} + \vec{\ell} \quad \vec{J} = 3 + \vec{\ell}$$

$^{22}\text{Ne}(\alpha, n)^{25}\text{Mg}$

C Massimi *et al.* (The n_TOF Collaboration), [Phys. Rev. C 85, 044615 \(2012\)](#)
 C Massimi *et al.* (The n_TOF Collaboration), [Phys. Lett. B 768, 1 \(2017\)](#)



E_n (keV)	E_x (keV)	E_α^{Lab} (keV)	J^π (\hbar)	Γ_γ (eV)	Γ_n (eV)
→ 19.92(1)	11112	589	2 ⁺	1.37(6)	2095(5)
62.73(1)	11154		1 ⁺	4.4(5)	7(2)
→ 72.82(1)	11163	649	2 ⁺	2.8(2)	5310(50)
→ 79.23(1)	11169	656	3 ⁻ (<i>a</i>)	3.3(2)	1940(20)
81.11(1)	11171			5(1)	1 – 30
100.33(2)	11190		3 ⁺	1.3(2)	5230(30)
155.83(2)	11243		2 ⁻	4.7(5)	5950(50)
→ 187.95(2)	11274	779	2 ⁺	2.2(2)	410(10)
→ 194.01(2)	11280	786	3 ⁻ (<i>a</i>)	0.3(1)	1810(20)
199.84(2)	11285		2 ⁻	4.8(4)	1030(30)
203.88(4)	11289			0.9(3)	3 – 20
210.23(3)	11295		2 ⁻	6.6(6)	7370(60)
→ 243.98(2)	11328	843	2 ⁺ (<i>b</i>)	2.2(3)	171(6)
260.84(8)	11344			1.0(2)	300 – 3900
261.20(2)	11344		> 3	3.0(3)	6000 – 9000

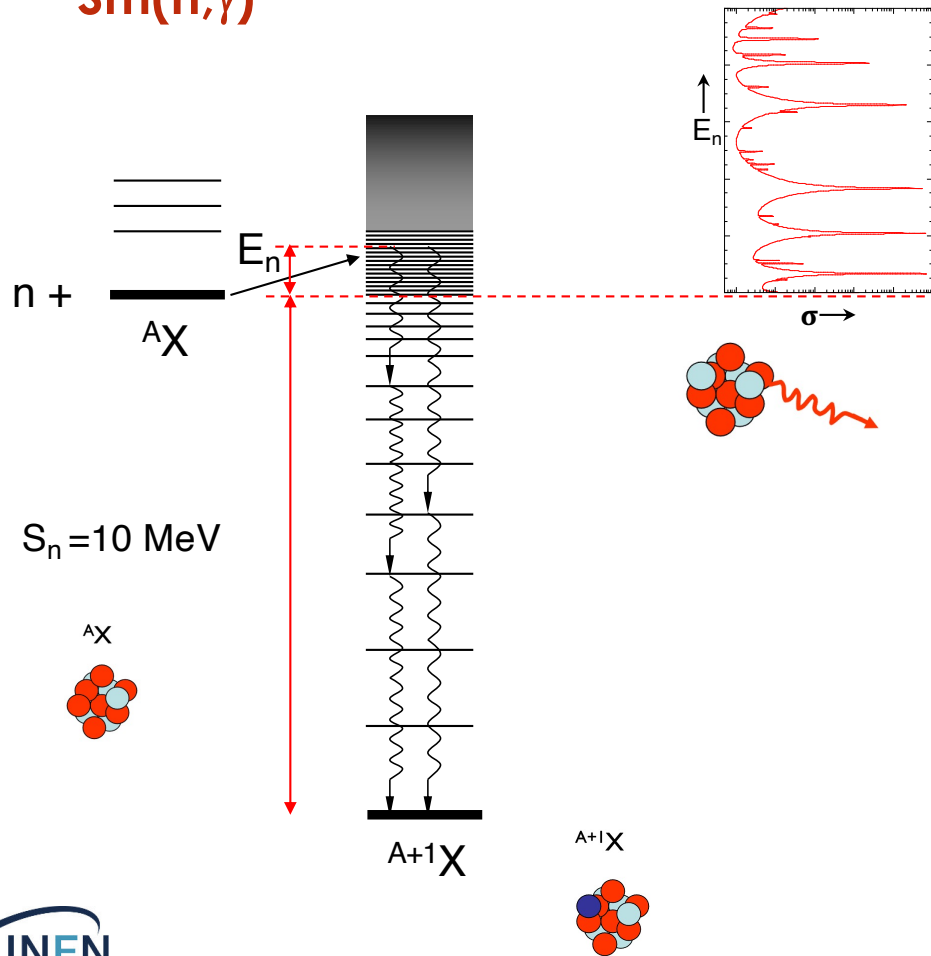


- ❖ Indirect approach, resonances above n -threshold
- ❖ R-Matrix parametrization ($E_R, \Gamma_\gamma, \Gamma_n, J^\pi$)
- ❖ Deduced ^{26}Mg states with natural parity



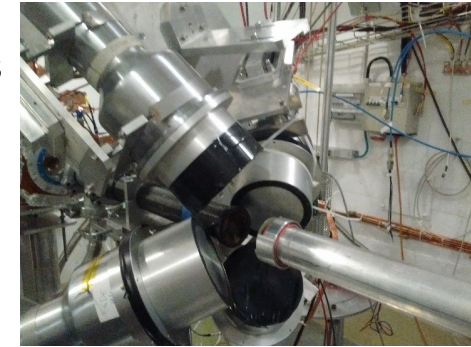
- ❖ No experimental Γ_α

$^{151}\text{Sm}(n,\gamma)$



The C_6D_6 Total Energy Detectors (TED)

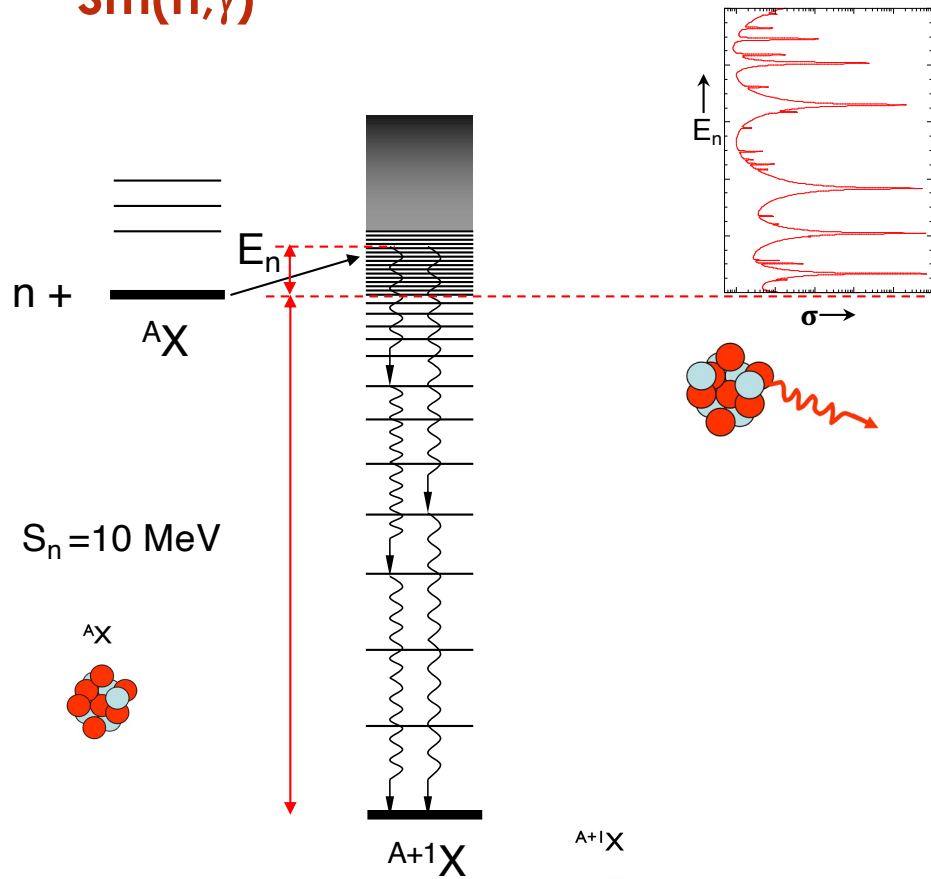
4 x C_6D_6 scintillators
 135°: in-beam γ -rays



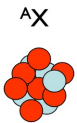
Efficiency to detect a cascade **UNKNOWN**:
 depends on the cascade path



$^{151}\text{Sm}(n,\gamma)$



$S_n = 10 \text{ MeV}$

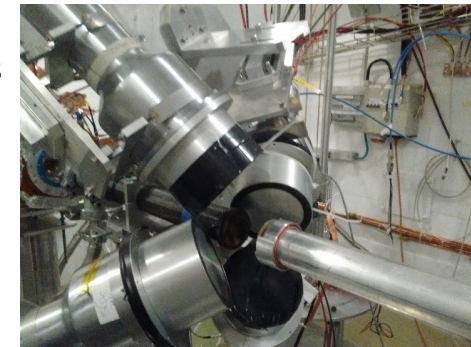


$A+1X$



The C_6D_6 Total Energy Detectors (TED)

4 x C_6D_6 scintillators
 135°: in-beam γ -rays

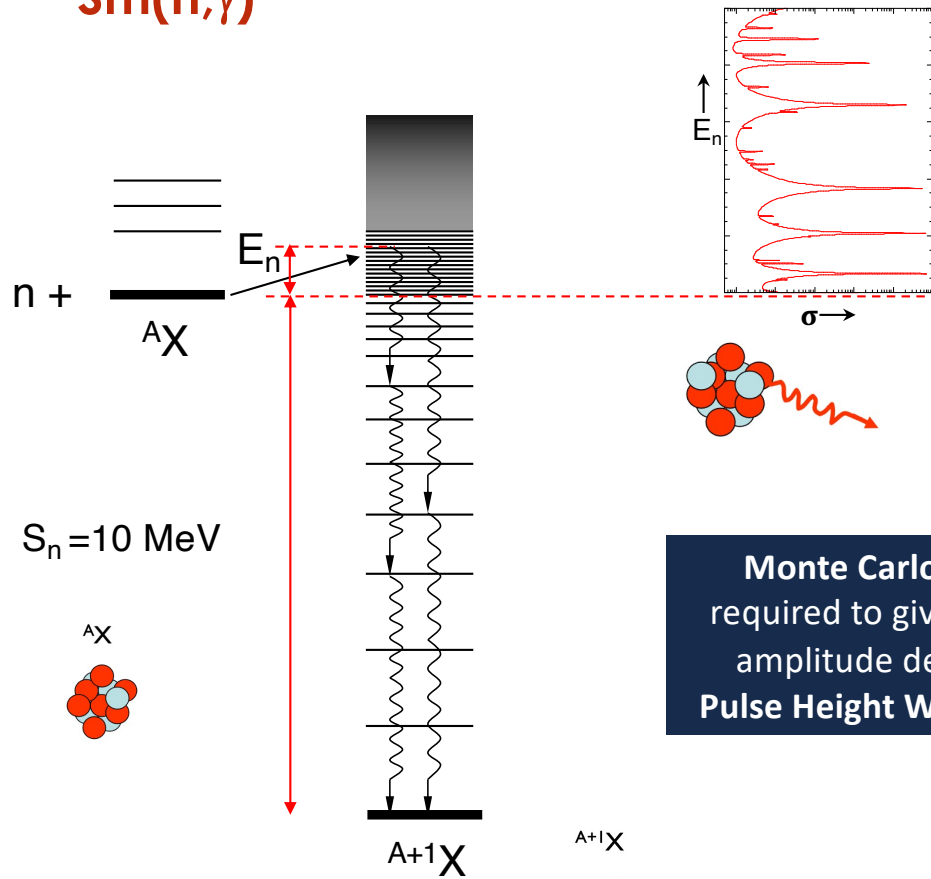


TED: Based in two principles

- **Condition I** : Low efficiency detectors $\epsilon_\gamma \ll 1$
 Detecting a cascade: $\epsilon_c = 1 - P(1 - \epsilon_\gamma) \approx \sum \epsilon_\gamma$
- **Condition II**: The efficiency is **proportional** to E_γ

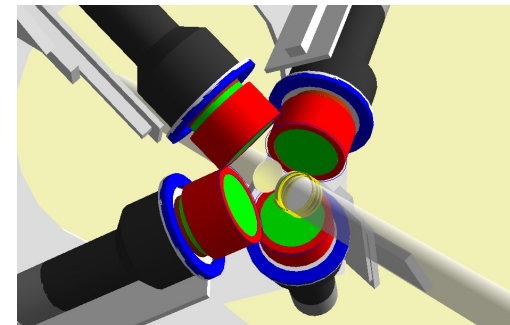
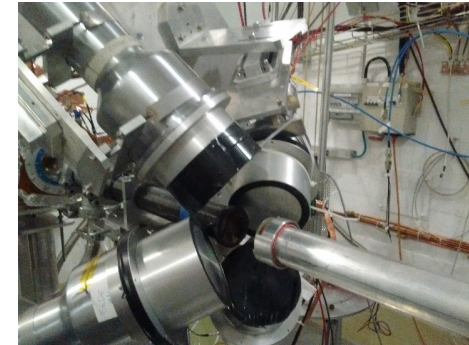
$$(\epsilon_c)_w = k \sum_{i=1} E_{\gamma_i} = k E_c$$

$^{151}\text{Sm}(n,\gamma)$



The C_6D_6 Total Energy Detectors (TED)

4 x C_6D_6 scintillators
 135°: in-beam γ -rays



Monte Carlo simulations are required to give to each signal an amplitude dependent weight:
Pulse Height Weighting Technique